INTERNATIONAL ATOMIC ENERGY AGENCY

NUCLEAR DATA SERVICES

DOCUMENTATION SERIES OF THE IAEA NUCLEAR DATA SECTION

IAEA-NDS-0233
May 2020

TENDL 2019
POINTWISE 2020
Temperature Dependent
Cross Section Library

by
Dermott E. Cullen
and
Jean-Christophe Sublet

Contact Information
Dermott E. Cullen
1466 Hudson Way
Livermore, CA 94550
USA
E.Mail: RedCullen1@comcast.net
Website: http://RedCullen1.net/HOMEPAGE.NEW

Jean-Christophe Sublet
International Atomic Energy Agency
P.O. Box 100, A-1400 Vienna
Austria

Abstract: This report presents results for a subset of n-TENDL-2019, including nuclear data only for incident neutrons, for 630 evaluations targets nuclides, Z=1-100, Hydrogen to Fermium, including as target some 28 m (1st) isomeric states. This subset represents the union of all targets for n-induced that exists in the currently available traditional libraries: JEFF-3.3, JENDL-4.0 and ENDF/B-VIII.0.

Nuclear Data Section
International Atomic Energy Agency
P.O. Box 100
A-1400 Vienna
Austria

E-mail: NDS.Contact-Point@iaea.org
Fax: (43-1)26007
Telephone: (43-1)2600-21725
Web: http://www-nds.iaea.org

Disclaimer

Neither the author nor anybody else makes any warranty, expressed or implied, or assumes any legal liability or responsibility for the accuracy, completeness or usefulness of any information disclosed, or represents that its use would not infringe privately owned rights.

The IAEA-NDS would appreciate any comment on this report at: NDS.Contact-Point@iaea.org.

The IAEA-NDS-reports should not be considered as formal publications. When a nuclear data library is sent out by the IAEA Nuclear Data Section, it will be accompanied by an IAEA-NDS-report which should give the data user all necessary documentation on contents, format and origin of the data library.

IAEA-NDS-reports are updated whenever there is additional information of relevance to the users of the data library.

For citations care should be taken that credit is given to the author of the data library and/or to the data center which issued the data library. The editor of the IAEA-NDS-report is usually not the author of the data library.

Acknowledgments

We thank Arjan Koning and Dimitri Rochman for supplying the TENDL 2019 data in the ENDF s30 format, used in this project. We thank Mark Baird (RSICC, Oak Ridge) for carefully handling and checking this report and data. We thank Nancy and Duane Larson, Bob MacFarlane, Maurice Greene, Pierre Ribon and, Mike Dunn, for their comparison of their cross section processing codes (SAMMY, NJOY, CALENDF and AMPX) against the PREPRO codes; these comparisons have led to significant improvements in the accuracy and reliability of the results produced by all five codes: SAMMY, NJOY, AMPX, CALENDF, PREPRO.

Vienna, May 2020

https://www-nds.iaea.org/

Table of Contents

I. TENDL-2019

I.1 What is TENDL-2019

The multipurpose, multifaceted methodical nuclear data libraries coded by TALYS [1], TARES [2,3], TANES, TAFIS, TEFAL and TASMAN as the Evaluated Nuclear Data Library TENDL [4] have been released nearly every year for the last decade. The 10th version is TENDL-2019 [5] which is based on both default and adjusted parameters of the most recent T6 codes and databases suite: TALYS-1.95, TAFIS, TANES (Fission observables), TARES-1.4 (Resolved and unresolved resonance parameters handler), TEFAL (ENDF-6 formatter) and TASMAN wrapping them all into a Bayesian Monte-Carlo (BMC) loop for uncertainty quantification. The T6 codes system combines BMC sampling methods according to the weight of its main nuclear model parameters and is uniquely capable of generating a full nuclear data library with complete covariances (model- and/or experiment-based), enabling thorough nuclear data uncertainty analysis that is not always possible using any other libraries or systems. When fed through application libraries [6] into modern simulation platform such as FISPACT-II [7,8] (a Bateman [9] solver) or MCNP [10], TRIPOLI [11], SERPENT [12], OpenMC [13] and CASMO [14] (as particle transport solvers), SPECTRA-PKA (primary knock-on atom evaluator) [15], its enhanced nuclear data primary and derived forms enable detailed, consistent and probing studies of the nuclear application landscape like no other, leading the way scientifically and technologically into uncharted territory.

TENDL-2019 now includes evaluated nuclear data for 2813 target nuclides, from Z=1-115, Hydrogen to Moscovium, including as target some 513 m (1st) and 30 n (2nd) isomeric states, all actually known with $T_{½} > 1$s, for seven incident particles: alpha, gamma, deuteron, proton, helium, triton and neutron, with incident energy up to 200 MeV. The 1 second limit is purely artificial but credible as very few applications would need targets with shorter half-life. The 200 MeV upper incident energy bound is achieved by assembling the formatted file in two concurrent format frames: the traditional detailed reactions frame up to 30 MeV, the transition energy whilst above it, all is lumped in a single reaction channels combined with light particles (A<4) and production radionuclides yields and spectra stored in MF-6 MT-5 from incident energies 30 to 200 MeV.

TENDL-2019 as a true general purpose library in its s30 form describes all open reaction channels in MF-1,2,3,8,9,10, product yields, spectra in MF-6, emitted spectra in MF-4,5,6 and short-lived daughter radionuclides (with half- lives $T_{½} > 0.1$s) and includes complete variance-covariance information in MF-32-35 derived from reference input parameters variation. When used in conjunction with the experimental database EXFOR, its primary differential and integral data forms (single, double differential cross-sections, emitted particles angular distribution and spectra) and some other data form such as kerma, heating, gas production can be compared with and if available experimental information [16] or other data libraries forms [17]. Others quite useful application forms such as, temperatures dependent cross section, Bondarenko or probability based self-shielding factors, tabulated angular distribution and emitted spectra can be extracted through the many processing steps allowed by its physics and format completeness.

I.2 What is TENDL-2019: neutron induced data

This report presents results for a subset of n-TENDL-2019 s30, including nuclear data only for incident neutrons, for 630 evaluations targets nuclides, Z=1-100, Hydrogen to Fermium, including as target some 28 m (1_{st}) isomeric states. This subset represents the union of all targets for n-induced that exists in the currently available traditional libraries: JEFF-3.3, JENDL-4.0 and ENDF/B-VIII.0. It would also be fair to say that the technological processes behind TENDL as described above are better equipped to model target above Z=12, Magnesium whilst if bridging all fissile targets, it cannot yet achieve the quality required for the traditional applications. It is why not all evaluations are yet independent as the 24 following files are taken from ENDF/B-VIII.0: $_{1,2,3}$H, $_{3,4}$He, $_{6,7}$Li, $_{10,11}$B, $_{7,9}$Be, $_{12,13}$C, $_{14,15}$N, $_{16,17,18}$O, $_{19}$F, $_{232}$Th, $_{233,235,238}$U and $_{239}$Pu, mainly but not only to conserve fission reactors criticality realizations. It also means that in contrast to the 606 original TENDL-2019 s30 files, the 24 targets above are in their original lesser format frame.

II. Overview

This report is similar to the series of "POINT" [18, 19, 20, 21, 22] reports that over the years have presented temperature dependent cross sections for the then current version of ENDF/B [23, 24]; this report is the first release of data based on TENDL [5], here named POINTWISE. In each case I (D.E.Cullen) have used my personal computer at home and publicly available data and codes:

1) Publicly available nuclear data (the current TENDL-2019 data, available on-line at https://tendl.web.psi.ch/tendl_2019/tendl2019.html) and,

2) Publicly available computer codes (the current PREPRO codes, available on-line at the Nuclear Data Section, IAEA, Vienna, Austria, https://www-nds.iaea.org/public/endf/prepro/) and

3) My own personal computer located in my home.

I have used these in combination to produce the temperature dependent cross sections used in applications and described in this report. We should mention that today anyone with a personal computer can produce these useful results: by its very nature we consider this data to be born in the public domain.

III. POINTWISE 2020

Below is a table defining the 630 neutron-induced TENDL 2019 evaluations included here. Each evaluation is identified by its atomic number (Z), chemical symbol (SS), and atomic mass number (A), and possibly isomer I.D. (m), e.g., 1-H-1, 92-U-238, 48-Cd-115m, etc. The tables are in ascending Z, A, m, order.

Table I. 1-H -1 through 54-Xe-123

1-H -1	20-Ca-47	31-Ga-69	40-Zr-94	48-Cd-107
1-H -2	20-Ca-48	31-Ga-70	40-Zr-95	48-Cd-108
1-H -3	21-Sc-44	31-Ga-71	40-Zr-96	48-Cd-109
2-He-3	21-Sc-45	32-Ge-70	41-Nb-91	48-Cd-110
2-He-4	21-Sc-46	32-Ge-71	41-Nb-92	48-Cd-111
3-Li-6	21-Sc-47	32-Ge-72	41-Nb-93	48-Cd-112
3-Li-7	21-Sc-48	32-Ge-73	41-Nb-94	48-Cd-113
4-Be-7	22-Ti-44	32-Ge-74	41-Nb-94m	48-Cd-114
4-Be-9	22-Ti-46	32-Ge-75	41-Nb-95	48-Cd-115m
5-B -10	22-Ti-47	32-Ge-76	42-Mo-92	48-Cd-116
5-B -11	22-Ti-48	33-As-71	42-Mo-93	49-In-113
6-C -12	22-Ti-49	33-As-72	42-Mo-94	49-In-114
6-C -13	22-Ti-50	33-As-73	42-Mo-95	49-In-115
7-N -14	23-V -48	33-As-74	42-Mo-96	50-Sn-112
7-N -15	23-V -49	33-As-75	42-Mo-97	50-Sn-113
8-O -16	23-V -50	33-As-76	42-Mo-98	50-Sn-114
8-O -17	23-V -51	33-As-77	42-Mo-99	50-Sn-115
8-O -18	24-Cr-50	34-Se-74	42-Mo-100	50-Sn-116
9-F -19	24-Cr-51	34-Se-75	43-Tc-96	50-Sn-117
10-Ne-20	24-Cr-52	34-Se-76	43-Tc-97	50-Sn-118
10-Ne-21	24-Cr-53	34-Se-77	43-Tc-98	50-Sn-119
10-Ne-22	24-Cr-54	34-Se-78	43-Tc-99	50-Sn-120
11-Na-22	25-Mn-52	34-Se-79	44-Ru-96	50-Sn-121
11-Na-23	25-Mn-53	34-Se-80	44-Ru-97	50-Sn-121m
12-Mg-24	25-Mn-54	34-Se-81	44-Ru-98	50-Sn-122
12-Mg-25	25-Mn-55	34-Se-82	44-Ru-99	50-Sn-123
12-Mg-26	26-Fe-54	35-Br-77	44-Ru-100	50-Sn-124
12-Mg-27	26-Fe-55	35-Br-79	44-Ru-101	50-Sn-125
13-Al-26	26-Fe-56	35-Br-80	44-Ru-102	50-Sn-126
13-Al-26m	26-Fe-57	35-Br-81	44-Ru-103	51-Sb-121
13-Al-27	26-Fe-58	35-Br-82	44-Ru-104	51-Sb-122
14-Si-28	26-Fe-59	36-Kr-78	44-Ru-105	51-Sb-123
14-Si-29	26-Fe-60	36-Kr-79	44-Ru-106	51-Sb-124
14-Si-30	27-Co-56	36-Kr-80	45-Rh-99	51-Sb-125
14-Si-31	27-Co-57	36-Kr-81	45-Rh-101	51-Sb-126
14-Si-32	27-Co-58	36-Kr-82	45-Rh-102	51-Sb-127
15-P -31	27-Co-58m	36-Kr-83	45-Rh-103	52-Te-120
15-P -32	27-Co-59	36-Kr-84	45-Rh-104	52-Te-121
15-P -33	27-Co-60	36-Kr-85	45-Rh-105	52-Te-121m
16-S -32	27-Co-62m	36-Kr-86	46-Pd-102	52-Te-122
16-S -33	28-Ni-56	37-Rb-85	46-Pd-103	52-Te-123
16-S -34	28-Ni-57	37-Rb-86	46-Pd-104	52-Te-124
16-S -35	28-Ni-58	37-Rb-87	46-Pd-105	52-Te-125
16-S -36	28-Ni-59	37-Rb-88	46-Pd-106	52-Te-126
17-Cl-35	28-Ni-60	38-Sr-83	46-Pd-107	52-Te-127m
17-Cl-36	28-Ni-61	38-Sr-84	46-Pd-108	52-Te-128
17-Cl-37	28-Ni-62	38-Sr-85	46-Pd-109	52-Te-129m
18-Ar-36	28-Ni-63	38-Sr-86	46-Pd-110	52-Te-130
18-Ar-37	28-Ni-64	38-Sr-87	47-Ag-106m	52-Te-131
18-Ar-38	28-Ni-66	38-Sr-88	47-Ag-107	52-Te-131m
18-Ar-39	29-Cu-63	38-Sr-89	47-Ag-108	52-Te-132
18-Ar-40	29-Cu-64	38-Sr-90	47-Ag-109	53-I -126
18-Ar-41	29-Cu-65	39-Y -87	47-Ag-110	53-I -127
19-K -39	29-Cu-66	39-Y -88	47-Ag-110m	53-I -128
19-K -40	29-Cu-67	39-Y -89	47-Ag-111	53-I -129
19-K -41	30-Zn-64	39-Y -90	47-Ag-112	53-I -130
20-Ca-40	30-Zn-65	39-Y -91	47-Ag-113	53-I -131
20-Ca-41	30-Zn-66	40-Zr-88	47-Ag-114	53-I -132
20-Ca-42	30-Zn-67	40-Zr-89	47-Ag-115	53-I -132m
20-Ca-43	30-Zn-68	40-Zr-90	47-Ag-116	53-I -133
20-Ca-44	30-Zn-69	40-Zr-91	47-Ag-117	53-I -134
20-Ca-45	30-Zn-70	40-Zr-92	47-Ag-118m	53-I -135
20-Ca-46	31-Ga-67	40-Zr-93	48-Cd-106	54-Xe-123

Table II. 54-Xe-124 through 100-Fm-255

54-Xe-124	61-Pm-149	68-Er-170	78-Pt-190	92-U -237
54-Xe-125	61-Pm-150	68-Er-171	78-Pt-191	92-U -238
54-Xe-126	61-Pm-151	68-Er-172	78-Pt-192	92-U -239
54-Xe-127	62-Sm-144	69-Tm-168	78-Pt-193	92-U -240
54-Xe-128	62-Sm-145	69-Tm-169	78-Pt-194	92-U -241
54-Xe-129	62-Sm-146	69-Tm-170	78-Pt-195	93-Np-234
54-Xe-130	62-Sm-147	69-Tm-171	78-Pt-196	93-Np-235
54-Xe-131	62-Sm-148	70-Yb-168	78-Pt-197	93-Np-236
54-Xe-132	62-Sm-149	70-Yb-169	78-Pt-198	93-Np-236m
54-Xe-133	62-Sm-150	70-Yb-170	79-Au-197	93-Np-237
54-Xe-134	62-Sm-151	70-Yb-171	80-Hg-196	93-Np-238
54-Xe-135	62-Sm-152	70-Yb-172	80-Hg-197	93-Np-239
54-Xe-135m	62-Sm-153	70-Yb-173	80-Hg-197m	94-Pu-236
54-Xe-136	62-Sm-154	70-Yb-174	80-Hg-198	94-Pu-237
55-Cs-133	63-Eu-151	70-Yb-175	80-Hg-199	94-Pu-238
55-Cs-134	63-Eu-152	70-Yb-176	80-Hg-200	94-Pu-239
55-Cs-135	63-Eu-152m	71-Lu-173	80-Hg-201	94-Pu-240
55-Cs-136	63-Eu-153	71-Lu-174	80-Hg-202	94-Pu-241
55-Cs-137	63-Eu-154	71-Lu-175	80-Hg-203	94-Pu-242
56-Ba-130	63-Eu-155	71-Lu-176	80-Hg-204	94-Pu-243
56-Ba-131	63-Eu-156	71-Lu-177	81-Tl-202	94-Pu-244
56-Ba-132	63-Eu-157	72-Hf-174	81-Tl-203	94-Pu-245
56-Ba-133	64-Gd-148	72-Hf-175	81-Tl-204	94-Pu-246
56-Ba-134	64-Gd-149	72-Hf-176	81-Tl-205	95-Am-240
56-Ba-135	64-Gd-150	72-Hf-177	82-Pb-204	95-Am-241
56-Ba-136	64-Gd-151	72-Hf-178	82-Pb-205	95-Am-242
56-Ba-137	64-Gd-152	72-Hf-179	82-Pb-206	95-Am-242m
56-Ba-138	64-Gd-153	72-Hf-180	82-Pb-207	95-Am-243
56-Ba-139	64-Gd-154	72-Hf-181	82-Pb-208	95-Am-244
56-Ba-140	64-Gd-155	72-Hf-182	83-Bi-208	95-Am-244m
57-La-137	64-Gd-156	73-Ta-179	83-Bi-209	96-Cm-240
57-La-138	64-Gd-157	73-Ta-180	83-Bi-210	96-Cm-241
57-La-139	64-Gd-158	73-Ta-180m	83-Bi-210m	96-Cm-242
57-La-140	64-Gd-159	73-Ta-181	84-Po-208	96-Cm-243
58-Ce-136	64-Gd-160	73-Ta-182	84-Po-209	96-Cm-244
58-Ce-137	64-Gd-161	74-W -180	84-Po-210	96-Cm-245
58-Ce-137m	65-Tb-158	74-W -181	88-Ra-223	96-Cm-246
58-Ce-138	65-Tb-159	74-W -182	88-Ra-224	96-Cm-247
58-Ce-139	65-Tb-160	74-W -183	88-Ra-225	96-Cm-248
58-Ce-140	65-Tb-161	74-W -184	88-Ra-226	96-Cm-249
58-Ce-141	66-Dy-154	74-W -185	89-Ac-225	96-Cm-250
58-Ce-142	66-Dy-155	74-W -186	89-Ac-226	97-Bk-245
58-Ce-143	66-Dy-156	74-W -188	89-Ac-227	97-Bk-246
58-Ce-144	66-Dy-157	75-Re-185	90-Th-227	97-Bk-247
59-Pr-141	66-Dy-158	75-Re-186	90-Th-228	97-Bk-248
59-Pr-142	66-Dy-159	75-Re-186m	90-Th-229	97-Bk-249
59-Pr-143	66-Dy-160	75-Re-187	90-Th-230	97-Bk-250
60-Nd-142	66-Dy-161	75-Re-188	90-Th-231	98-Cf-246
60-Nd-143	66-Dy-162	76-Os-184	90-Th-232	98-Cf-247
60-Nd-144	66-Dy-163	76-Os-185	90-Th-233	98-Cf-248
60-Nd-145	66-Dy-164	76-Os-186	90-Th-234	98-Cf-249
60-Nd-146	66-Dy-165	76-Os-187	91-Pa-229	98-Cf-250
60-Nd-147	67-Ho-163	76-Os-188	91-Pa-230	98-Cf-251
60-Nd-148	67-Ho-165	76-Os-189	91-Pa-231	98-Cf-252
60-Nd-149	67-Ho-166m	76-Os-190	91-Pa-232	98-Cf-253
60-Nd-150	68-Er-162	76-Os-191	91-Pa-233	98-Cf-254
61-Pm-143	68-Er-163	76-Os-192	92-U -230	99-Es-251
61-Pm-144	68-Er-164	76-Os-193	92-U -231	99-Es-252
61-Pm-145	68-Er-165	77-Ir-190	92-U -232	99-Es-253
61-Pm-146	68-Er-166	77-Ir-191	92-U -233	99-Es-254
61-Pm-147	68-Er-167	77-Ir-192	92-U -234	99-Es-254m
61-Pm-148	68-Er-168	77-Ir-193	92-U -235	99-Es-255
61-Pm-148m	68-Er-169	77-Ir-194m	92-U -236	100-Fm-255

IV. PREPRO 2020 Codes

In addition to the changes in the basic TENDL 2019 evaluations, it should be noted that the current PREPRO 2020 [25] codes were used to process all of this data, and there have been significant improvements in the ENDF/B Pre-processing codes (PREPRO) used in earlier reports. The improvements were both in terms of improving the basic methods used by the codes and in terms of incorporating the latest ENDF-6 Formats and Procedures [24] used by the current evaluations. The result is more accurate cross section data throughout this TENDL 2019 - POINTWISE 2020 library.

WARNING – due to recent changes in ENDF-6 Formats and Procedures [24] only the latest version of the ENDF/B Pre-processing codes, namely PREPRO 2020 [25], can be used to accurately process all current TENDL 2019 evaluations [5]. If you fail to heed this warning and you use any earlier versions of these codes the results can be inaccurate/unpredictable.

The most recent PREPRO codes run on virtually any computer, and are available FREE on-line from the Nuclear Data Section, IAEA, Vienna, Austria, website at,

https://www-nds.iaea.org/public/endf/prepro/

IV.1 Data Processing

As distributed the TENDL 2019 original evaluated data [5] includes cross sections represented in the form of a combination of resonance parameters and/or tabulated energy dependent cross sections, nominally at 0 Kelvin temperature. For use in applications, this data has been processed using the 2020 version of the ENDF/B Pre-processing codes (PREPRO 2020) [25] to produce temperature dependent, linearly interpolable in energy, tabulated cross sections, in the ENDF-6 format [24].

For use in applications this library has been processed into the form of temperature dependent cross sections at five neutron reactor like temperatures, between 0 and 1200 Kelvin, in steps of 300 Kelvin (the exception being 293.6 Kelvin, for exact room temperature at 20 Celsius). It has also been processed to five astrophysics like temperatures between 1 eV and 80 keV. For reference purposes, 300 Kelvin is approximately 1/40 eV, so that 1 eV is approximately 12,000 Kelvin (twice the Sun photosphere temperature). At each temperature the cross sections are tabulated and linearly interpolable in energy.

The steps required, and codes used to produce room temperature, linearly interpolable tabulated cross sections, in the ENDF-6 format [24], are described below; the name of each code is given in parenthesis; for details of each code see reference [25].

Here are the steps and order in which PREPRO 2020 [25] codes were used.

1) Convert all data to a FORTRAN, C and C++ compatible format (**ENDF2C**)
2) Convert to Linearly interpolable, tabulated energy dependent cross sections (**LINEAR**)
3) Add the resonance contribution to cross sections (**RECENT**)
4) Doppler broaden all cross sections to each temperature (**SIGMA1**)
5) Check data, define redundant cross sections by summation (**FIXUP**)
6) Update evaluation dictionary in MF/MT=1/451 (**DICTIN**)

For the "cold" (0 Kelvin) data steps 1), 2), 3) and 5), 6) were used (no Doppler broadening). For the data at other temperatures, after steps 1), 2), 3), the data were Doppler broadened to each temperature using step 4), and the results were then made consistent with the ENDF/B formats and conventions [24] using steps 5) and 6), to produce the final distributed data. The result is linearly interpolable in energy, tabulated, temperature dependent cross sections, in the simple text ENDF-6 format, ready to be used in applications.

Note - this processing only involved the energy dependent neutron cross sections. All other data in the evaluations, e.g., angular and energy distributions, variance-covariance, etc. were not affected by this processing, and are identical in all versions of the results, i.e., it is the same for all temperatures, 0 K through 1200 K, and 1 eV through 80 keV. For compactness of storage these other data are only included once, as MFOther; here “Other” means other than ENDF MF=1 through 3, temperature dependent data.

IV.2 Accuracy or Uncertainty of Results

WARNING: PLEASE do not confuse the OVERALL UNCERTAINTY of the TENDL data with the additional uncertainty introduced by the PREPRO codes. We judge that the TENDL cross sections for any isotope, at any temperature and incident neutron energy is not known to better than roughly 1%; we may know integrals more accurately, but not the detailed energy dependent cross sections. As such we have defined the additional uncertainty added by the PREPRO codes to be so small that they add essentially no additional uncertainty to the OVERALL uncertainty in the original ENDF/B formatted data.

Each of the codes described above that was used to process data to obtain tabulated, linearly interpolable in energy cross sections, processed the data to within a user defined accuracy, or allowable uncertainty. The ENDF Pre-processing codes (PREPRO) are self-documenting, in the sense that the ENDF formatted output data that each code produces includes comments at the beginning of each evaluation (MF/MT=1/451), defining the accuracy to which the cross sections were calculated. The combination of comments added by all of the codes defines the sequence and accuracy used by all of them. The accuracy is the same for all evaluations. Therefore, for exact details of the accuracy of the data, see the comments at the beginning of any evaluation. For use in POINTWISE 2020 (this report) all cross sections were reconstructed to within an accuracy of 0.01% in the thermal range, and 0.1 % at all other incident neutron energies and temperatures; this is beyond the accuracy to which this data in known, so we assume that the PREPRO data processing used to produce POINTWISE 2020 does not add any significant additional uncertainty

to the inherent overall uncertainty of the data. For data testing purposes this is important for users to understand this point.

IV.3 Content of the Library

This library includes neutron induced evaluations from the TENDL 2019 s30 neutron induced general purpose library. The above tables summarize the contents of this library. This library contains evaluations for 630 materials; all are isotopes of elements Z=1 through 100, but be aware that data is not necessarily included for all elements, Z = 1 through 100; see the above table for a summary.

This POINTWISE 2020 library does not contain data from special purpose ENDF/B libraries, such as fission products, thermal scattering, photon interaction data, etc. To obtain any of these special purpose libraries contact the National Nuclear Data Centers.

The POINTWISE 2020 library include each of the 630 evaluations is stored as a separate file. The data are in the simple text ENDF-6 format, which allows the data to be easily transported between computers. The entire library requires approximately 4 gigabytes of storage in compressed form; once uncompressed the data for each temperature requires roughly a gigabyte.

This library contains data for some metastable materials, which are indicated by an "m" at the end of their name, e.g., ZA052131.M = 52-Te-131m

Most of the 630 evaluations are complete, in the sense that they include all cross sections over the energy range 10^{-5} eV to at least 20 MeV; mostly to 30 MeV and most extend up to 200 MeV.

The POINTWISE 2020 webpage is compressed; when uncompressed you will find a single directory named POINT2020 containing twelve (12) sub-directories,

DOCUMENT - A copy of this report in MSWord and PDF formats.
0K - 0 Kelvin cross sections
293.6K - 293.6 Kelvin cross sections
600K - 600 Kelvin cross sections
900K - 900 Kelvin cross sections
1200K - 1200 Kelvin cross sections
1eV - 1 eV cross sections
1keV - 1 keV cross sections
5keV - 5 keV cross sections
30keV - 30 keV cross sections
80keV - 80 keV cross sections
MFOther - MF=4 through 99, temperature independent; same for ALL temperatures

Except for DOCUMENT, each of these directories contains 630 files, one file for each of the 630 evaluations. Each evaluation is a simple text file, 80 characters per line, and is a complete ENDF-6 "tape" [24], including a starting "tape" identification line, and ending with a "tape" end line [24]. In this simple text form, each file can be used by a wide variety of available computer codes that

treat data in the ENDF/B format, e.g., all the PREPRO codes.

IV.4 Requesting POINTWISE 2020 Data

Please do not contact the authors of this report to request this data; we do not have the resources necessary to directly respond to requests for this data. This data has been distributed and is Internationally available from nuclear data/code centers throughout the World,

1) Within the United States: contact the National Nuclear Data Center, Brookhaven National Laboratory, services@bnlnd2.dne.bnl.gov
2) Within Western Europe: contact the OECD Nuclear Energy Agency/ Data Bank (NEA/DB), Paris, France, programs@nea.fr

Otherwise: contact the Nuclear Data Section, International Atomic Energy Agency, Vienna, Austria at nds.contact-point@iaea.org and https://www-nds.iaea.org/

IV.5 Installation and Use of POINTWISE 2020

We recommend that you,

1) Copy the single compressed POINTWISE 2020 file to your computer,
2) Uncompress and un-tar the file; then delete the compressed and tar files.
3) You should then have one directory named POINT2020 containing all the data
4) To randomly access the data, execute (double click) POINT2020.htm.

The main POINTWISE 2020 directory will contain the twelve (12) sub-directories, described above. These POINTWISE 2020 directories include HTML routines to allow interactive retrieval of the data. Once uncompressed the result will be a directory of about 15 gigabytes. To put that in perspective, today it costs less than $0.10 U.S. to purchase, install, and maintain on-line one gigabyte of disk storage. Therefore, the cost of maintaining this 15 gigabyte library on-line is trivial.

IV.6 FORTRAN, C, C++ Compatible ENDF numerical results

I have added the **ENDF2C** code to PREPRO, to ensure that ALL PREPRO output in the simple text ENDF format are completely FORTRAN, C and C++ compatible. Currently evaluated data even from major code centers are still not completely FORTRAN, C and C++ compatible. Therefore, when I begin pre-processing any evaluation the first PREPRO code I run is **ENDF2C** to ensure that ALL ENDF formatted output in subsequent codes are completely compatible. This is a very simple, but very important step: it would be such a shame if after all the effort invested to produce accurate results it cannot be accurately read and used by application codes. If you use PREPRO codes it as STRONGLY recommended that you ALWAYS first use **ENDF2C** so that you will be able to avoid this problem. PREPRO also uses the current ENDF convention that sequence numbers start at 1 for each section (MAT/MF/MT), instead of the older convention starting at 1 for each material (MAT).

Before ENDF2C

```
1.002000+3 1.996800+0          0          0          0          0 128 3  1  125
0.000000+0 0.000000+0          0          0          1        149 128 3  1  126
       149          2                                              128 3  1  127
1.000000-5 3.420300+0 1.000000-4 3.403000+0 2.530000-2 3.395510+0 128 3  1  128
1.000000+2 3.395010+0 1.000000+3 3.394900+0 2.000000+3 3.394800+0 128 3  1  129
3.000000+3 3.394400+0 4.000000+3 3.389400+0 5.000000+3 3.385000+0 128 3  1  130
1.000000+4 3.367000+0 2.000000+4 3.342000+0 3.000000+4 3.321000+0 128 3  1  131
4.000000+4 3.302000+0 5.000002+4 3.285000+0 6.000002+4 3.270000+0 128 3  1  132
```

After ENDF2C

```
1002.00000 1.99680000          0          0          0          0 128 3  1    1
0.0        0.0                 0          0          1        149 128 3  1    2
       149          2                                              128 3  1    3
.000010000 3.42030000 .000100000 3.40300000 .025300000 3.39551000 128 3  1    4
100.000000 3.39501000 1000.00000 3.39490000 2000.00000 3.39480000 128 3  1    5
3000.00000 3.39440000 4000.00000 3.38940000 5000.00000 3.38500000 128 3  1    6
10000.0000 3.36700000 20000.0000 3.34200000 30000.0000 3.32100000 128 3  1    7
40000.0000 3.30200000 50000.0200 3.28500000 60000.0200 3.27000000 128 3  1    8
```

Note that in the above example we can see that the numerical values are EXACTY the same in both cases. However, the ENDF2C output include 9 digits of precision, and is completely FORTRAN, C and C++ compatible. In comparison the ENDF 7-digit, so called “E-less” data, such as 1.234567+3 (as opposed to 1234.56789) is not standard in any computer language and can lead to errors in interpretation when codes attempt to read this data, particularly, C, C++….codes.

IV.7 PREPRO uses 9- or 10-digits precision for all ENDF output

As an example, consider: 9 digits: 12324.56789, versus 7 digits: 1.234567+3. Here we can see that the 9 digit output is a hundred times more precise compared to the 7 digit output. This is very important for narrow milli-eV wide resonances in the keV or today even in the MeV energy range. Below I show the difference between PREPRO output data using 9 or 10 digits of accuracy compared to STANEF using 7 digits. To see the real danger of using 7-digit output with today's modern evaluations let's see what happens when we run the 9-digit RECENT output through STANEF and truncate it to 7-digits.

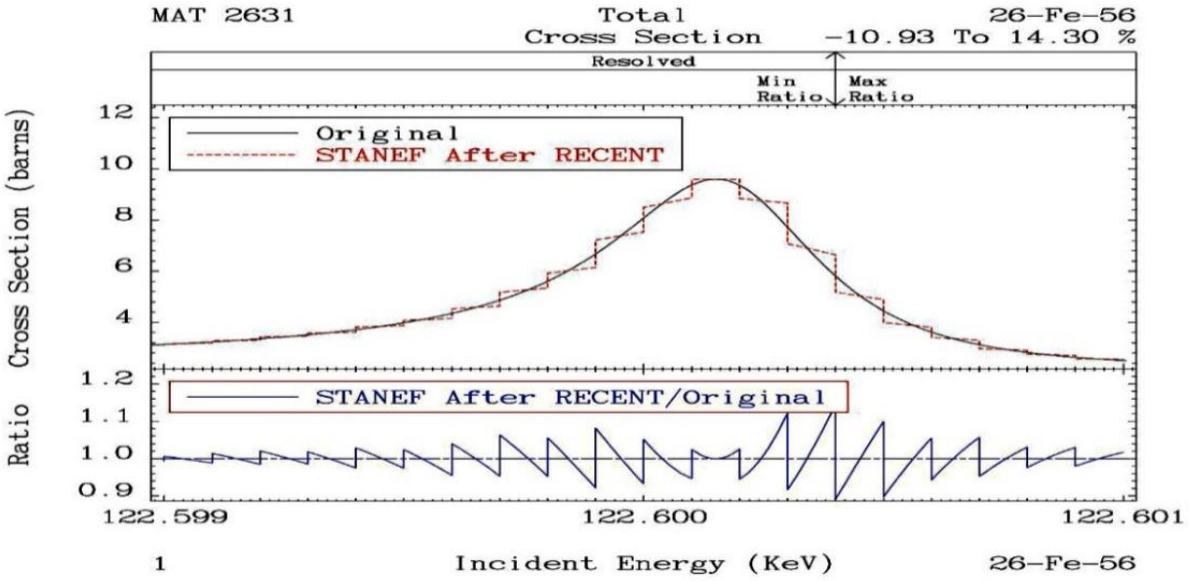

Figure 1 Total showing differences up to14.3% differences

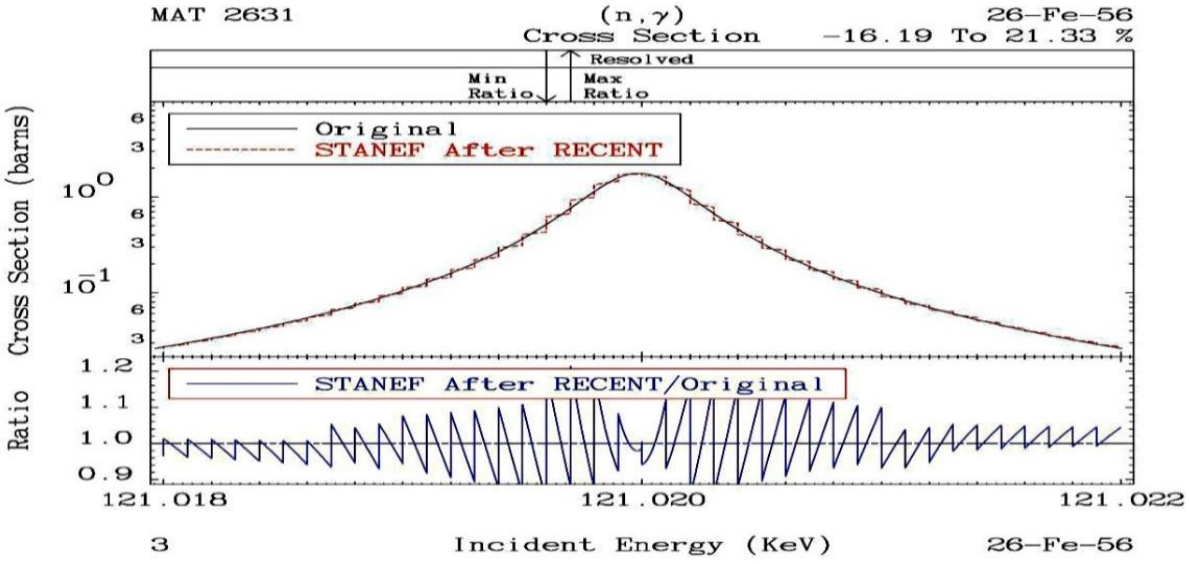

Figure 2 Capture showing differences up to 21.3% difference

Here we see that the 7-digit output is unable to accurately define the shape of these resonances – this is IMPORTANT to understand, so let me repeat: it is PHYSICALLY IMPOSSIBLE with only 7 digits. Rather than the smooth profile produced by the RECENT 9-digit output, the 7-digit STANEF output produces Ziggurats = stepped pyramids. To understand the problem we need merely compare the 9-digit RECENT output near the peak of the resonance,

```
122600.007 8.18440080 122600.018 8.34734256 122600.021 8.391426722631 3  1 6030
122600.028 8.49343634 122600.055 8.86885730 122600.077 9.139853322631 3  1 6031
122600.099 9.36221564 122600.120 9.51387393 122600.131 9.565109362631 3  1 6032
122600.142 9.59483076 122600.153 9.60178112 122600.164 9.585085692631 3  1 6033
122600.176 9.53939892 122600.178 9.52899291 122600.180 9.517793222631 3  1 6034
122600.182 9.50580250 122600.184 9.49302393 122600.196 9.400050502631 3  1 6035
122600.207 9.29106975 122600.218 9.16076388 122600.229 9.010880802631 3  1 6036
122600.240 8.84348060 122600.251 8.66085453 122600.261 8.483667022631 3  1 6037
122600.283 8.06587838 122600.305 7.62540465 122600.319 7.341331292631 3  1 6038
122600.332 7.07896654 122600.354 6.64519685 122600.375 6.250366772631 3  1 6039
122600.397 5.86278292 122600.419 5.50514627 122600.441 5.178659552631 3  1 6040
122600.462 4.89577103 122600.484 4.62825344 122600.505 4.398676332631 3  1 6041
122600.527 4.18301692 122600.549 3.99047205 122600.571 3.818722112631 3  1 6042
122600.592 3.67214930 122600.614 3.53482178 122600.625 3.471802962631 3  1 6043
122600.636 3.41225491 122600.658 3.30276311 122600.679 3.209061382631 3  1 6044
122600.701 3.12093801 122600.722 3.04533219 122600.744 2.974035832631 3  1 6045
122600.766 2.90992540 122600.788 2.85219006 122600.809 2.802371112631 3  1 6046
122600.831 2.75512041 122600.853 2.71238188 122600.875 2.673669622631 3  1 6047
122600.896 2.64007944 122600.918 2.60804847 122600.939 2.580185982631 3  1 6048
122600.961 2.55355301 122600.983 2.52927697 122601.005 2.507124522631 3  1 6049
```

To the STANEF 7-digit output over the same energy range,

```
1.226000+5 8.184401+0 1.226000+5 8.347343+0 1.226000+5 8.391427+02631 3  1 4518
1.226000+5 8.493436+0 1.226001+5 8.868857+0 1.226001+5 9.139853+02631 3  1 4519
1.226001+5 9.362216+0 1.226001+5 9.513874+0 1.226001+5 9.565109+02631 3  1 4520
1.226001+5 9.594831+0 1.226002+5 9.601781+0 1.226002+5 9.585086+02631 3  1 4521
1.226002+5 9.539399+0 1.226002+5 9.528993+0 1.226002+5 9.517793+02631 3  1 4522
1.226002+5 9.505802+0 1.226002+5 9.493024+0 1.226002+5 9.400051+02631 3  1 4523
1.226002+5 9.291070+0 1.226002+5 9.160764+0 1.226002+5 9.010881+02631 3  1 4524
1.226002+5 8.843481+0 1.226003+5 8.660855+0 1.226003+5 8.483667+02631 3  1 4525
1.226003+5 8.065878+0 1.226003+5 7.625405+0 1.226003+5 7.341331+02631 3  1 4526
1.226003+5 7.078967+0 1.226004+5 6.645197+0 1.226004+5 6.250367+02631 3  1 4527
1.226004+5 5.862783+0 1.226004+5 5.505146+0 1.226004+5 5.178660+02631 3  1 4528
1.226005+5 4.895771+0 1.226005+5 4.628253+0 1.226005+5 4.398676+02631 3  1 4529
1.226005+5 4.183017+0 1.226005+5 3.990472+0 1.226006+5 3.818722+02631 3  1 4530
1.226006+5 3.672149+0 1.226006+5 3.534822+0 1.226006+5 3.471803+02631 3  1 4531
1.226006+5 3.412255+0 1.226007+5 3.302763+0 1.226007+5 3.209061+02631 3  1 4532
1.226007+5 3.120938+0 1.226007+5 3.045332+0 1.226007+5 2.974036+02631 3  1 4533
1.226008+5 2.909925+0 1.226008+5 2.852190+0 1.226008+5 2.802371+02631 3  1 4534
1.226008+5 2.755120+0 1.226009+5 2.712382+0 1.226009+5 2.673670+02631 3  1 4535
1.226009+5 2.640079+0 1.226009+5 2.608048+0 1.226009+5 2.580186+02631 3  1 4536
1.226010+5 2.553553+0 1.226010+5 2.529277+0 1.226010+5 2.507125+02631 3  1 4537
```

Here the entire shape of the resonance is between 122.599 keV and 122.601 keV, and we can see that all the above tabulated points in both tables start with EXACTLY the same six digit energy 122600. This means that with 9-digit RECENT output we only have three digits with which to define the entire shape of the resonance, which is adequate, but with 7-digit STANEF output we only have one digit!!!!, which is far from adequate. Compare what should be EXACTLY the same energy points that I have highlighted, and you will see smooth variation of the 9-digit RECENT energies, but ALL OF THE HIGHLIGHTED 7-DIGIT STANEF ENERGIS ARE EXACTLY THE SAME VALUE, 1226600.2 eV, which is what is causing the Ziggurats (stepped pyramids) that we see in the above figures = a constant X value (energy) and a range of Y values (cross

sections), creating a vertical STEP in the above figure = nonsense, completely due to nothing but truncating to 7-digit energies.

The bottom line here is to understand that due to the details included in modern evaluations it is physically impossible for 7-digit output to accurately represent the energy dependent cross sections to anywhere near our target allowable uncertainty (0.1%). In this case we find differences in the total of over 14% and in capture over 21%; see the above plots = 140 to 210 times our target uncertainty of 0.1%. Be aware that these are not isolated differences in a few resonances; we see these differences over the entire resolved resonance energy range, and this isn't even the worse case, e.g., the latest Fe56 evaluation includes resonances well up into the MeV range, an order of magnitude higher in energy than the resonances shown in the above figures. Below is but one example of a capture resonance in the MeV range where truncating from 9-digits to 7-digits results in differences of up to 226% = over a factor of 2!!!!!

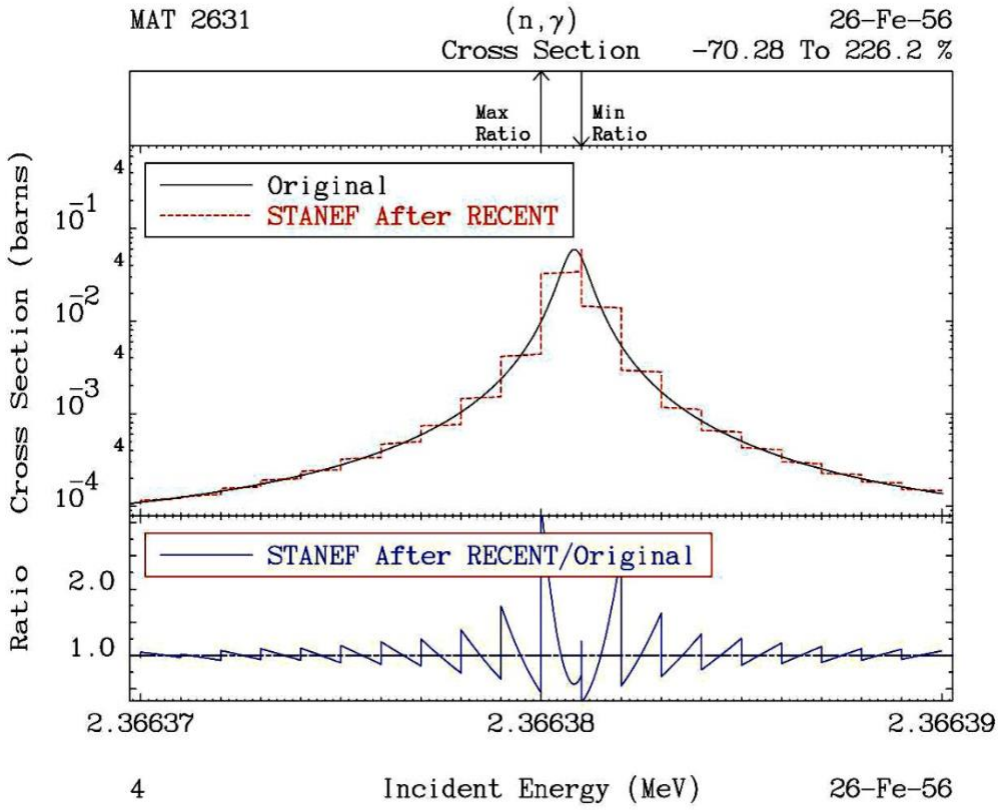

Figure 3 The impact of 7 or 9 significant digits

IV.8 Improved BEST Input Parameters

Based on extensive use of the earlier versions of the PREPRO codes over many years we have been able to define the BEST Input Parameters to use with these codes. Of particular note is that simply decreasing the minimum cross section from 10^{-10} to 10^{-30} barns to be linearized (tabulated data below the minimum are copied, ignoring the ENDF interpolation code). This has a rather dramatic effect, particularly on (neutron, charged particle) reactions, which often have long, slowly decreasing tails toward the reaction threshold. In the below example the evaluator tabulated values of the cross sections down to below 10^{-20} barns using log-log interpolation (INT=5). Earlier versions of PREPRO ignored the interpolation code below 10^{-10} and copied the original tabulated values and indicated lin-lin interpolation (INT=2). In contrast today using the BEST input PREPRO linearized the cross sections over the entire tabulated range. Here the cross section can be quite small, but extend over a large energy range, so there might be an integral effect; in the below plot interpolated values differ by up to a factor of 1 million. Since this extension has only a minor effect on the overall size of the pre-processed ENDF data (i.e., the number of tabulated energy points is roughly the same), there is virtually no penalty in accurately including these data.

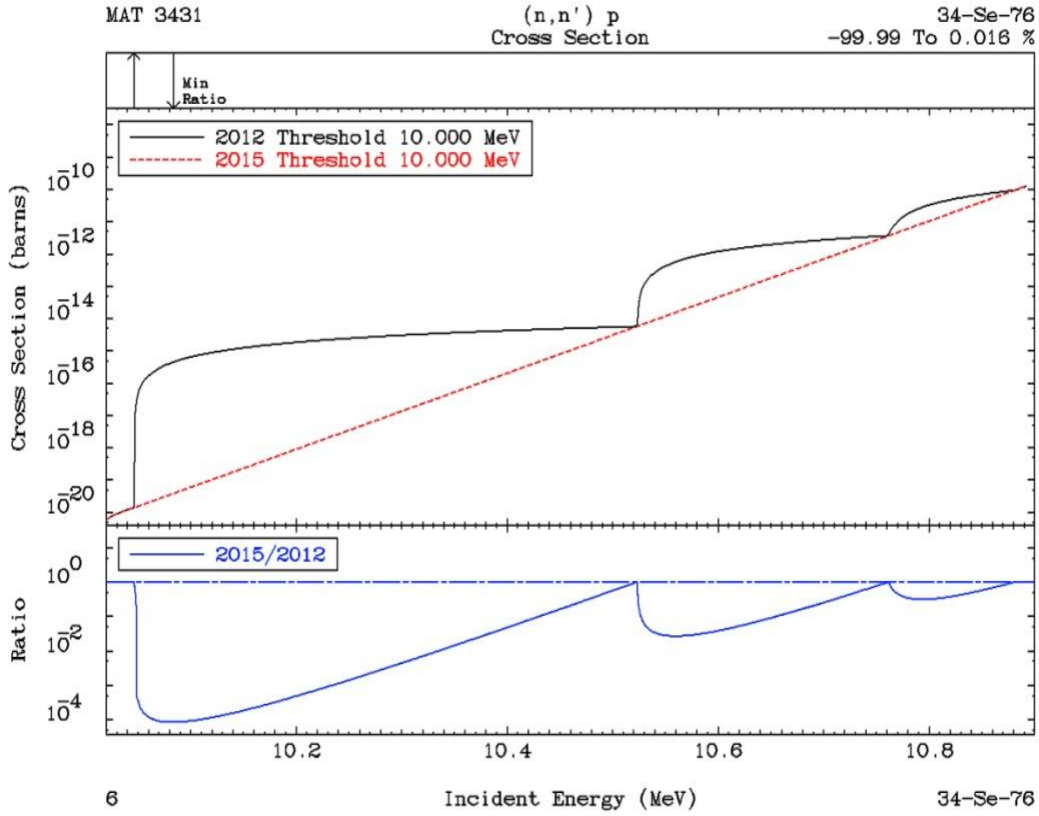

Figure 4 The impact of interpolation laws

V. Doppler Broadening

V.1 The Effects of Temperature and Doppler Broadening

For those readers who are not familiar with the effects of temperature and Doppler broadening on neutron cross sections and transport, for details I suggest that you read references [25, 26, 27, 28]. Here I will give a brief description of these effects. Users of neutron cross sections, should be aware that there are several important effects of temperature and Doppler broadening,

First an important point to understand is that: neutron cross sections ARE NOT TEMPRATURE DEPENDENT, that I to say in the relative frame-of-reference at the same relative speed the cross sections are temperature INDEPENDENT. However, normally we do not perform our calculations in the relative frame-of-reference; we perform our calculations in the Laboratory frame-of-reference, and it is our transformation to the LAB frame that makes neutron cross sections "appear" to be temperature dependent. This problem of relative motion is quite similar to the "apparent" rotation of the Sun about the Earth, that led to mankind assuming the Earth was the center of the Universe for thousands of years. In the LAB frame-of-reference we have a similar problem in that the thermal motion of atoms within any material can change the RELATIVE speed between a neutron and a target atom, and this effect will depend on how fast the atoms within the material are moving, and this SPEED of the atoms is directly related to the TEMPERATURE of the medium. If you read references such as [25, 26, 27, 28], you will see that they are using exactly the same basic cross sections at all temperatures (the temperature independent, relative frame data), but in order to define the LAB frame-of-reference cross sections we need, they average over the thermal motion of the atoms in the material in order to define the average cross section "seen" (encountered) by a neutron with any given LAB speed.

As far as the effect of temperatures, first I will mention the well known effect in the neutron resonance region, where as the temperature increases resonances become broader, hence the name Doppler broadening. Figure 5 top below illustrates the effect of temperature on the U^{238} capture cross section for neutron reactor like temperatures, and figure 5 bottom illustrates this effect for astrophysical like temperatures. These figures each contain four sub-figures, with each sub-figure comparing cross sections at two progressively higher temperatures. In figure 5 each sub-figure shows exactly the same incident neutron LAB energy and cross section range. From these figures we can see that as temperature increases the peaks of the resonances become lower, and the minima between resonances become higher. At extremely high temperature the entire resonance structure disappears, and the cross section approaches a simple 1/v shape (where v is the neutron speed) (see, ref. 11 for an explanation). This temperature effect will have a very important effect on resonance self-shielding in any neutron transport calculation. You should note from these figures that due to the large resonance spacing in U_{238} the resonance structure can still be seen up to very high temperatures.

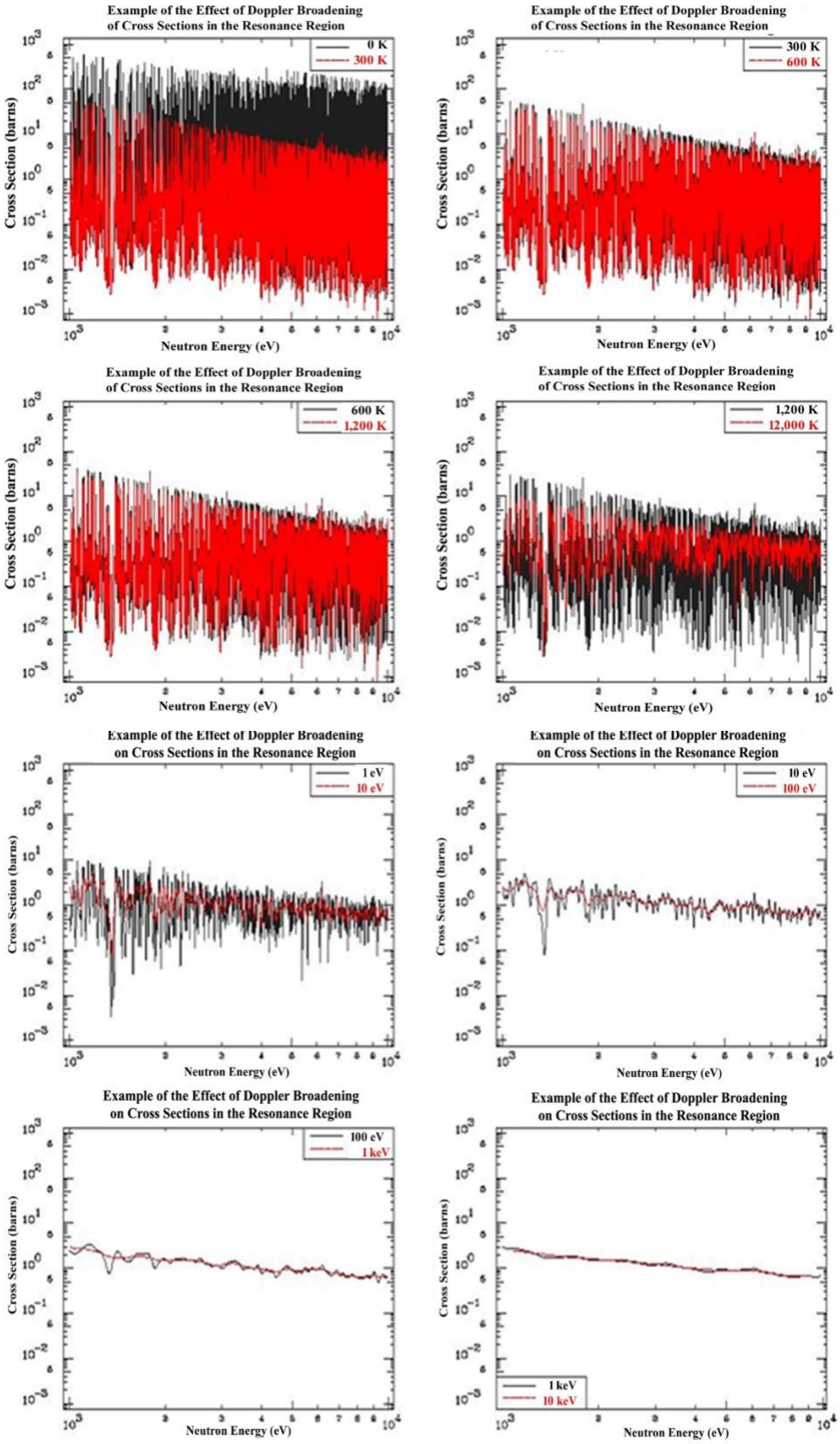

Figure 5 Effect of Doppler broadening in the resonance range of cross sections

To understand the importance of considering temperature we should consider reaction rates, such as captures/second, in various systems. In optically thin systems (few mean free paths dimensions) the flux will be unshielded, and our reaction rates will be defined by a simple cross section average,

Unshielded Capture = $\int_{E1}^{E2}[\Sigma c(E)\phi(E)]dE$ = capture cross section times neutron flux

In optically thick systems (many mean free paths dimensions) the flux will be shielded (the flux is suppressed by the total cross section) and our reaction rates must include the effect of self-shielding on the cross section average,

Shielded Capture = $\int_{E1}^{E2}[\Sigma c(E)\phi(E)/\Sigma t(E)]dE$ = including one over total cross section

Consider for example the U238 capture cross section in the incident neutron energy between 1 and 10 keV as shown in fig. 5. If we calculate the unshielded and shielded average capture cross section for the energy interval over the range of temperatures shown in fig. 5, we obtain the results shown below in the below table.

What we see from these results is that the unshielded average capture cross section is virtually independent of temperature, being about 1 barn over the entire temperature range. In contrast the shielded average cross section varying by over a factor of three between the 0 K average (0.293 barns) and the 10 keV average (0.939 barns). The point to learn from this is that without including the effect of self-shielding in multi-group calculations, temperature has very little effect on the average cross sections, which is quite simply wrong for optically thick systems.

Effect of Temperature on Average Cross Sections

Temp.	Unshielded (barns)	Shielded (barns)
0 K	0.996	0.293
293.6 K	0.966	0.526
600 K	0.996	0.576
1,200 K	0.996	0.630
12,000 K (1 eV)	0.996	0.799
10 eV	0.998	0.905
100 eV	1.000	0.933
1 keV	1.004	0.935
10 keV	1.007	0.939

Another, less well known, effect of Doppler broadening is at lower energies where as temperature increases the low energy constant scattering cross section increases and at very low energies approaches a simple 1/v shape (where v is the neutron speed); this effect is explained in detail in ref [28]. Figure 3 illustrates the effect of temperature on the hydrogen total cross section. From this figure we can see that starting from a “cold” (0 Kelvin) cross section that is constant at about 20 barns, as temperature increases the cross section increases. Compared to the “cold” 20 barn

cross section, at thermal energy the Doppler broadened cross section is about 30 barns, i.e., 50 % higher. Note also from this figure that this effect extends well above thermal energy. For example, at 293.6 Kelvin the thermal energy is 0.0253 eV, but we can see this effect up to about 1 eV; a factor of 400 higher in energy. From the lower half of figure 6 we can see that at very low energy the cross section approaches a simple 1/v shape (where v is the neutron speed) and the cross sections at various temperatures become proportional to one another. This effect on the cross sections at low energy is very important for thermal and low energy neutron systems.

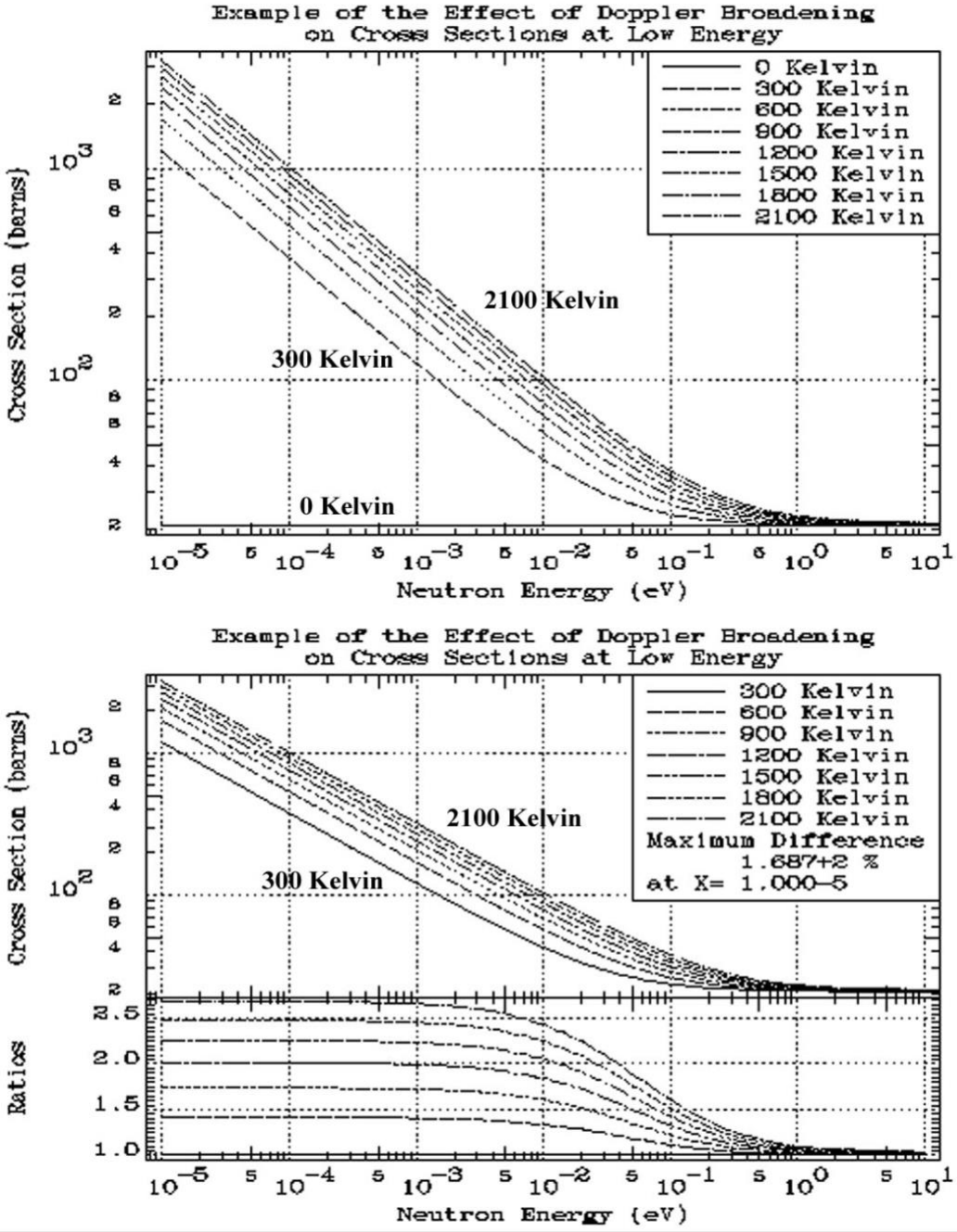

Figure 6 Effect of Doppler broadening on resonance cross sections at low energy

Yet another important effect of temperature is that at lower energies neutrons do not slow down in energy as quickly and neutron scatter can even result in the upscatter of neutrons, i.e., when neutrons scatter they can gain, rather than lose, energy. This is a well known effect at low energies, where thermal scattering law data or a free gas model is used to describe the interaction of neutrons with target atoms that are moving about with thermal motion [28]. Figure 7 illustrates the effect of temperature on the neutron spectrum over a wide range of temperatures. This effect can also be important at higher energies, particularly near narrow resonances, where thermal motion of the target atoms can cause neutrons to slightly upscatter, but even slight upscatter can cause a neutron to scatter from below to above the energy of a very narrow resonance. See reference [25], for a routine designed to be used in conjunction with the SIGMA1 method of Doppler broadening [26], to handle neutron thermal scattering. This routine [26] is completely compatible for use with the cross sections included here, since these cross sections were Doppler broadened using the SIGMA1 method [25]. The combination of SIGMA1 [25] Doppler broadened cross sections and THERMAL [27] to handle thermal scattering, is currently used in the TART Monte Carlo transport code [29].

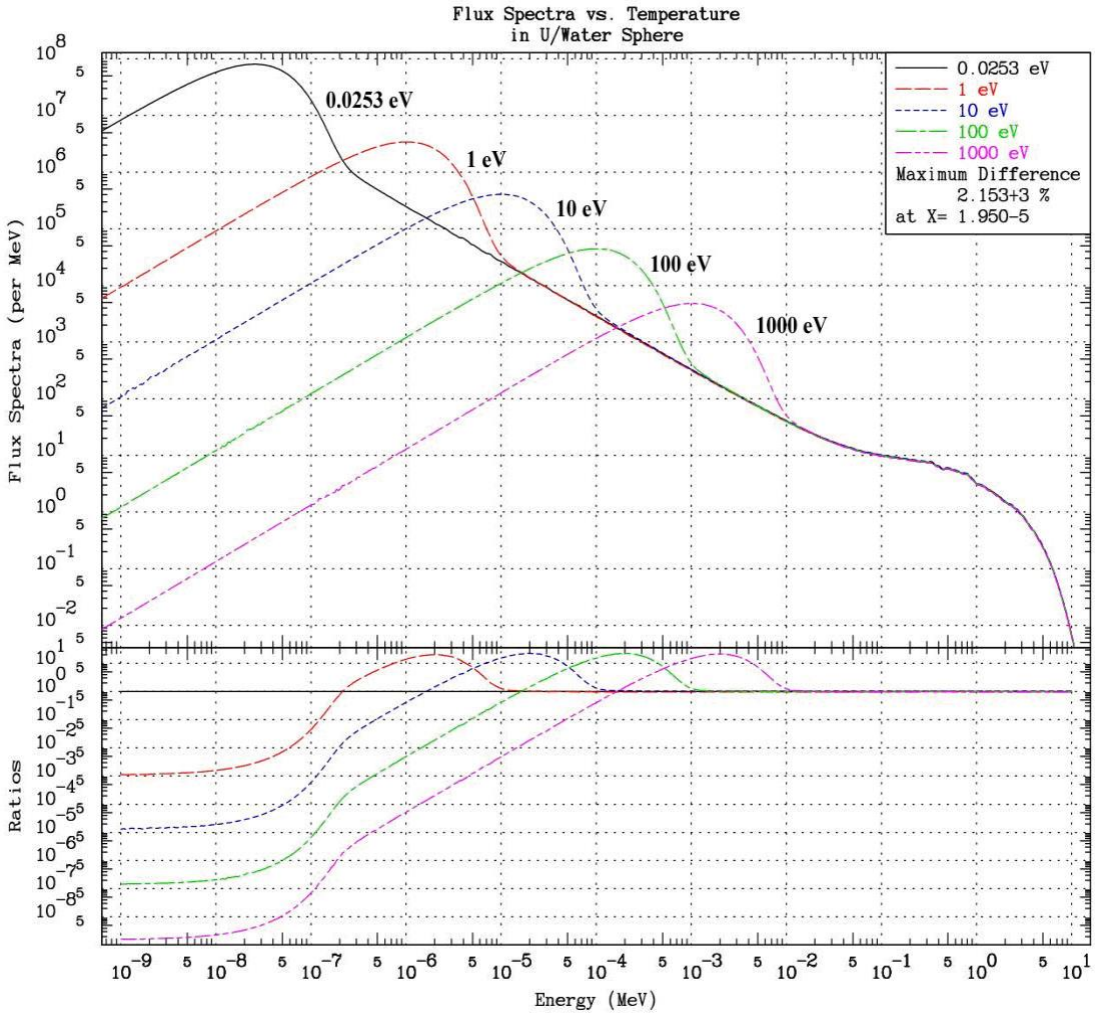

Figure 7 Effect of Doppler broadening on neutron spectrum

VI. Doppler Broadening Update

VI.1 Introduction

In the following section the concept of Doppler broadening is introduced. This discussion will be limited to the effect of Doppler broadening due to so-called free atoms. We will only briefly discuss thermal scattering law data, that includes binding effects, such as vibration and rotation of crystals. These binding effects are not included in the Doppler broadening method used for this report, and beyond the scope of this report, and as such will not be discussed here in detail.

Here emphasis will be placed on the role that Doppler broadening plays for broadening of neutron-induced cross sections at fission reactor temperatures, particularly in the resonance region. However, for generality, we will also cover higher temperature fusion and astrophysics applications, involving free atom neutron and charged particle-induced cross sections.

VI.2 What causes Doppler broadening?

Let us first repeat the most important point to understand free atom cross sections are not temperature dependent. That is to say, the cross sections for the same relative speed between a projectile (neutron) and a target atom are independent of temperature. This assumption is explicitly included in the Doppler broadening equation we use here. Note, that this is not true for thermal scattering law data, where temperature can affect binding, i.e., the physics are very different.

Although the cross section in the relative frame of reference is not temperature dependent, the Boltzmann equation that we solve using our transport codes is expressed in the laboratory frame-of-reference, rather than the relative frame between neutron and target nuclei. It is because we want to perform our calculations in the laboratory frame-of-reference that requires us to define our cross sections in the same frame-of-reference, and it is solely due to the necessity to transform data from the relative to laboratory frame-of-reference that forces us to include Doppler broadening of cross sections.

The cross section or probability of a neutron interacting with any given nucleus depends on the relative speed between the neutron and the nucleus. In neutron transport usually neutron energy rather than speed is used and evaluated data libraries [24] present cross sections and resonance parameter as a function of incident neutron energy, where the neutron energy is measured relative to stationary target nuclei. However, the transport equation describes neutrons in the laboratory frame of reference, and therefore in order to solve this equation, we must define cross sections in the same frame of reference. If all of the nuclei in a medium were stationary (a so called “cold” medium), then the energy of the neutron in the laboratory system would be exactly equal to the energy measured to the energy measured relative to the nuclei in the medium, i.e., in this case the relative and lab frames of references coincide.. In this case the evaluated data as presented in evaluated libraries are exactly what we need for use in the transport equation. However, in any real case, the nuclei in a medium will have a distribution of kinetic energies and will be moving about in a random manner. In this case, for any given neutron energy in the laboratory system, there will not be one unique neutron energy, measured relative to the distribution of randomly moving nuclei, rather there will be an entire spectrum of relative energies.

Visualize a neutron with a laboratory energy corresponding to the peak energy of a resonance, incident upon a medium in which the nuclei are moving about due to thermal agitation. Since the nuclei are moving about, there is a probability that the nucleus that the neutron actually interacts with is moving either toward or away from the neutron before the collision; this would cause the relative energy of the neutron to either increase or decrease, respectively. Since here we assumed the neutron was incident with a laboratory energy corresponding to the peak of the resonance, if the relative energy is lower or higher than this value, the cross section that the neutron actually encounters will be lower than the peak value. Of course, there is also a probability that the neutron will interact with a nucleus such that its relative energy is identical to the peak of the resonance. We must consider not one neutron interacting with one nucleus, but rather the average due to an ensemble of neutrons interacting with the ensemble of nuclei within the medium. It is easy to see that in the case of this example if we consider neutrons incident with a laboratory energy corresponding to the peak of a resonance, the average cross section that they encounter will actually be less than the cross section corresponding to the peak of the resonance. Therefore, when the nuclei are moving about due to thermal agitation, the cross section that a neutron of a given laboratory energy encounters will be different from the cold (0 Kelvin) cross sections.

To further complicate the situation, when the bulk temperature of the medium changes, the kinetic energy of the nuclei in the medium changes, which changes the distribution of relative speeds, or energy, between a neutron of a given laboratory energy and the nuclei in the medium. Therefore, we should expect the effects that we see to depend upon the temperature of the medium. If we are to solve our transport equation in the laboratory system, we must somehow reduce this complicated situation to define a single "equivalent" laboratory frame-of-reference cross section**.**

In what sense should our cross section in the laboratory frame-of-reference be "equivalent" to what is happening in the relative frame-of-reference? What we are interested in conserving is what we can observe in either frame of reference. We cannot observe neutrons, flux or barns directly. We can only observe when neutrons interact with the medium; in other words, we can only observe reactions. Therefore, we will define our laboratory frame-of-reference cross sections in order to assure that the number of reactions per unit time will be the same in either system. In the following discussion, this laboratory frame-of-reference cross section will simply be referred to as the Doppler broadened cross section.

VI.3 The Doppler Broadening Equation

In any real medium at a temperature above absolute zero, the target nuclei are in thermal agitation and possess a distribution of velocities. Here the relative speed (V_R) between a monoenergetic beam of neutrons incident upon the medium and the nuclei within the medium will also be distributed. In such a medium we must define our laboratory cross section to agree with the observed reaction rate. However, because the cross section is determined by the relative speed, as opposed to the laboratory speed of the neutron, the Doppler broadened cross section will not generally be the same as the cold cross section. The observed reaction rate per unit neutron will be,

Lab reactions = Relative reactions

$$R(V,T) = V\sigma(V,T) = \int_{[Vt;Vr>0]} R(V_r,0)p(\overline{V}_T)d\overline{V}_T = \int_{[Vt;Vr>0]} V_r\sigma(V_r,0)p(\overline{V}_T)d\overline{V}_T$$

Since here $p(\overline{V}_T)d\overline{V}_T$ is a normalized distribution, it is obvious from this equation that if the reaction rate $V_r\sigma(V_r,0)$ is constant the broadened cross section $V\sigma(V,T)$ will also be constant, independent of temperature, regardless of the model, $p(\overline{V}_T)d\overline{V}_T$, used to describe the thermal motion of the target nuclei. That is to say a 1/V cross section will be independent of temperature. It has been demonstrated elsewhere that a 1/V cross section is the only cross section shape that is independent of temperature. Therefore, in all other cases we must consider Doppler broadening, since we expect the laboratory cross section to be temperature dependent.

From our earlier discussion of physically what causes Doppler broadening, it is easy to understand why a 1/V cross section is independent of temperature. In this case if we have a neutron with speed V that interacts with a nucleus such that the relative speed is V_r, the reaction rate observed will be exactly the same regardless of the value of V_r; the reaction rate will be exactly the same as if the interaction had occurred with a relative speed V, independent of the velocity distribution of the target nuclei. This is not true even for simple cross section shapes, such as a constant cross section, since in this case if the relative speed V_r is larger than V, the observed reaction rate will be larger and conversely it will be lower if V_r is smaller than V. It will be shown later in this work that these two effects of larger and smaller values of V_r do not quite balance out and a cold constant cross section is temperature dependent.

Assuming the distribution of free atoms can be accurately described by an isotropic Maxwellian distribution, $p(\overline{V}_T)d\overline{V}_T$, we obtain the familiar integral form of the Doppler broadening equation used by the SIGMA1 method, In terms of reaction rate, the equation can be written in the form,

$$VR(V,T2) = \left[\frac{1}{4\pi\tau}\right]^{1/2} \int_0^\infty VrR(Vr,T1)dVr \times \{Exp[-(V-Vr)^2/4\tau] - Exp[-(V+Vr)^2/4\tau]\}$$

$$\tau = \frac{k(T2-T1)}{2M}$$

By differentiating this can be shown to be mathematically analogous to the diffusion equation (age diffusion for neutrons or heat conduction) equation in an infinite, homogeneous, spherically symmetric system. In this analogy the familiar independent variables of space and time in the neutron or heat diffusion equation are equivalent in the Doppler broadening equation to the independent variables, neutron speed and temperature of the medium. Similarly, the normal dependent variable neutron flux or temperature is analogous to the dependent variable reaction rate in the Doppler broadening equation. The differential form of the Doppler broadening equation is,

$$\nabla^2 R(V,\tau) = \frac{\partial}{\partial\tau} R(V,\tau)$$

Where ∇^2 is the Laplacian operator in spherical coordinates,

$$\nabla_2 = \frac{1}{V}\frac{\partial}{\partial V}{}_2[\mathrm{VR}(\mathrm{V},\tau)]$$

and the "initial" condition is that $\mathrm{R}(\mathrm{V},\tau_1)$ is known for some initial value of $\tau = \tau_1$.

The main reason for demonstrating at this point that the Doppler broadening equation is simply the diffusion equation, is not because this is a simple or convenient starting point to solve the Doppler broadening equation; indeed trying to solve the differential form of this equation can lead to many numerical difficulties when applied to neutron cross sections. The main reason is to improve our understanding of the Doppler broadening process and to be able to simply predict what will happen to a cross section under Doppler broadening to successively higher temperatures by analogy to what happens to a temperature distribution at successively later times when we solve the diffusion equation.

VI.4 ENDF Format

The SIGMA1 method of Doppler broadening [25, 26] was developed specifically to meet the need of the then new ENDF format; in particular, tabulated cross section in the ENDF [24] format, MF=3, are by definition in the laboratory frame-of-reference, and the temperature of these tabulated cross sections are defined in the ENDF format in MF/MT=1/451.

VI.5 The Effects of Doppler broadening

The original SIGMA1 method [26] focused on the well known effect of doppler broadening free atom cross sections, namely broadening resonances in the resolved energy range [24]. Up to the time SIGMA1 was developed there were a variety of methods used, such as psi-chi [30, 21, 32], that only included the resonance region problem, and TEMPO [33], which is similar to SIGMA1 [25, 26], but none of these focused explicitly on the then newly designed ENDF format, nor did they include other important effects, which I describe below.

Let me again state: The SIGMA1 method [25, 26] was designed to start from LAB frame-of-reference, linearly interpolable, tabulated energy dependent free atom cross sections in the ENDF format at a starting temperature, and to produce Doppler broadened LAB frame-of-reference, linearly interpolable, tabulated energy dependent cross sections in the ENDF format at any higher temperature.

In my original SIGMA1 paper [26] I demonstrated that the Doppler broadening equation is the diffusion equation for the REACTION RATE, in spherical coordinates; in our case the more familiar diffusion equation variables of space and time, are replaced by neutron speed and temperature. This is a very important point, because there is a wealth of literature concerning the diffusion equation that can be used to better understand and solve the problem we are dealing with.

One of the best known properties of the diffusion equation is that it is an initial value problem; As classically used this means we can start at any time and calculate results for advancing time, but we cannot go backwards in time; mathematically this is clear; physically this would violate the second law of thermodynamics, by attempting to create order out of chaos. In this case it means that we can start at any temperature, and calculate results at any higher temperature, but we cannot calculate results at any lower temperature, e.g., we cannot uniquely un-Doppler broaden cross sections. Below I illustrate the problem any experimental faces when they measure temperature

broadened cross sections, even for room temperature measurements. Based on a room temperature measurement we cannot uniquely un-broaden cross sections (illustrated below). The best we can do is GUESS at resonance parameters, reconstruct the cold (0 K) cross sections, doppler broaden them to the same temperature as the measurement, and see how well – or poorly – the GUESS agrees with the measurement (It is important to understand that in doing this we are not un-broadening). This may not be theoretically very satisfying, but it does meet the needs of many ENDF applications. Why? Because we know from the properties of the diffusion equation, we cannot uniquely define the cross section at lower temperatures, but if the GUESS agrees well at room temperature we can uniquely define the cross section of higher temperatures, which in many applications is all we are interested in, e.g., designing refrigerators being an exception.

VI.6 Doppler Broadening Resolved Resonances

Below I illustrate a few examples of the effect of Doppler broadening on resonances in the resolved resonance region, figure 8 illustrate the U238 capture cross section, cold (0 Kelvin) compared to room temperature (293.6 Kelvin). It may surprise readers to see the effect this seemingly small temperature change has on the cross sections.

1) There is an enormous "smoothing" effect, e.g. from the ratio, shown as the lower third of this figure, we can see that the resonance peaks decrease by a factor of up to 100, and the minima between resonances increases by a similar amount of up to 100.
2) The effect of broadening to even 293.6 K, roughly 1/40 eV, extends all the way up in energy throughout the entire resolved resonance energy range , well in the keV energy range. The neutron energy may be in the keV range, but in this energy range U238 capture widths can be milli-eV wide, comparable to the thermal motion of target nuclei.

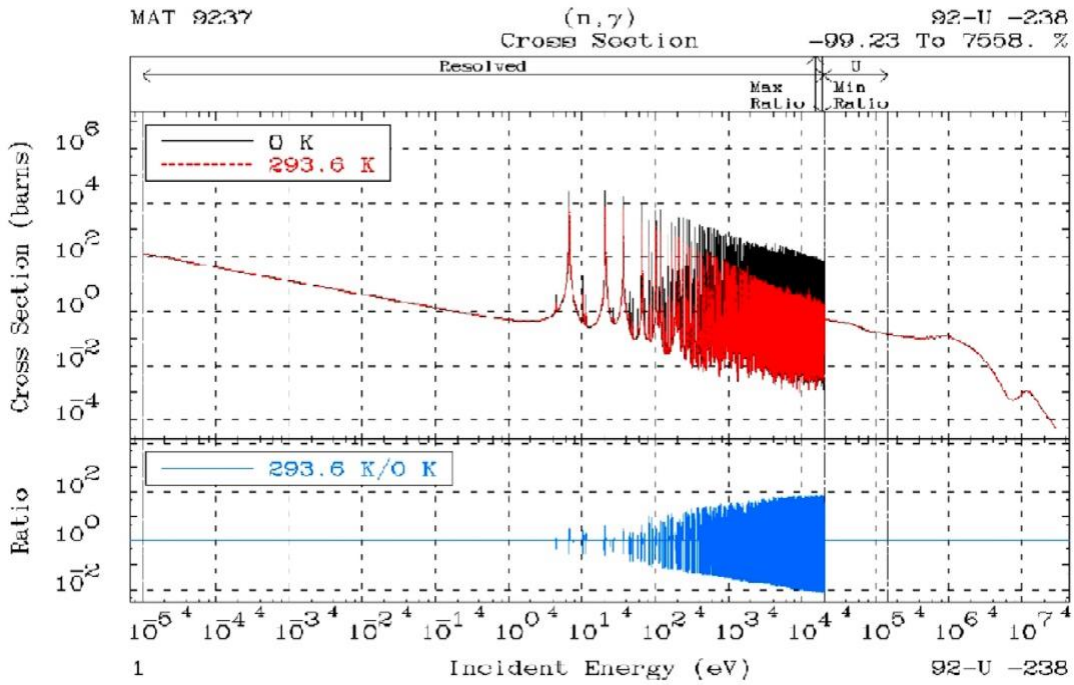

Figure 8 Broadening effects on resonances, above and below

Figure 9 illustrate a few more details of broadening the U238 capture cross section, over successfully smaller energy ranges, so we can see more details of the broadening; first a detail of the resolved resonance region from 100 eV up to 20 keV. Note, the ratio shown in the lower third of this figure: This shows the peaks of the resonances decreasing by up to a factor of 100, and the minimum between resonances increasing by up to a factor of 100.

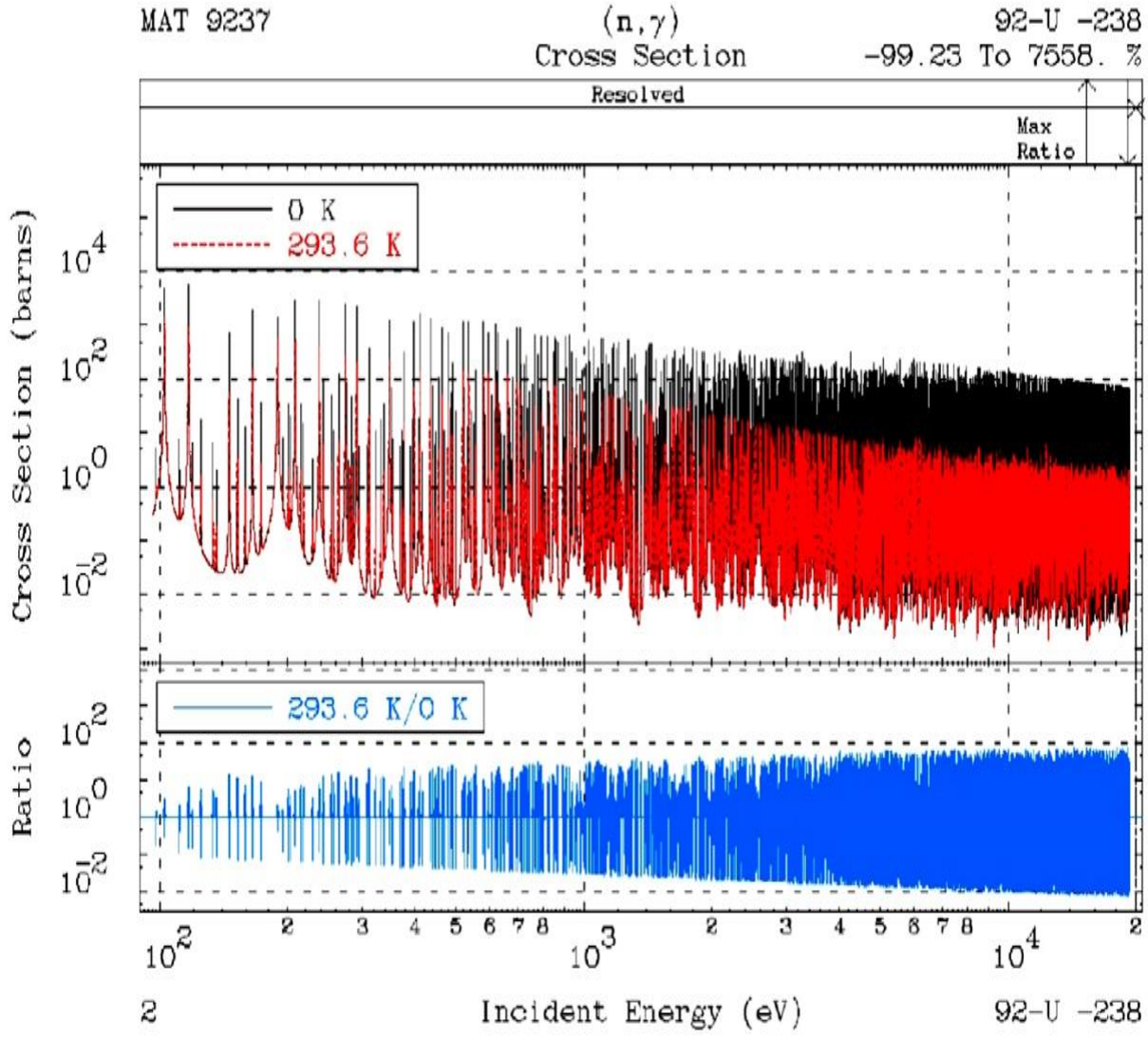

Figure 9 Broadening effects on resonances

Next more detail in figure 10 near 10 keV. Again, we can see the enormous differences in the range of the cross section, becoming smoother, decreasing peaks, and increasing minima between resonances.

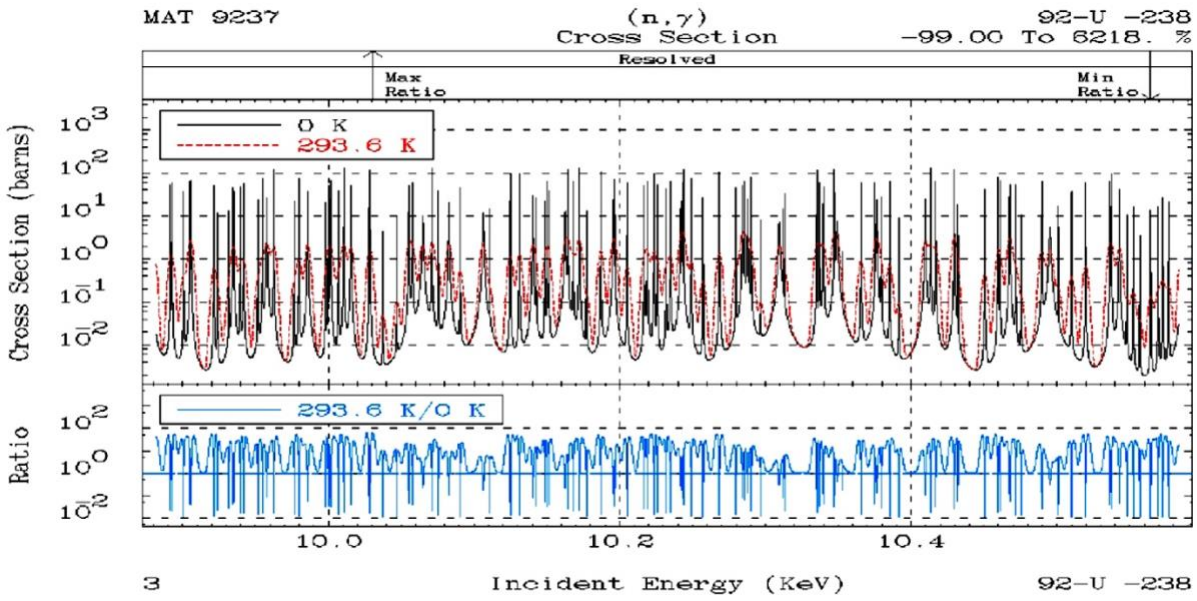

Figure 10 Broadening effects on resonances, zoom in

Figure 11 shows an extremely small energy range, where we can see the details of the effect of broadening on but a few of the capture resonances. This clearly illustrates the enormous effect that even this small temperature change (0 to 293.6 K) has on broadening these resonances.

Hopefully this also illustrates why we cannot use the Doppler broadening equation (the diffusion equation), to "un-broaden" cross sections. imagine an experimentalist measuring the room temperature cross section slightly below and above 10.54 keV (that's all the experiment shows). The broadened cross sections are so similar one would be hard pressed to realized that there are actually two resonance slightly below 10.54 keV, versus only one slightly above.

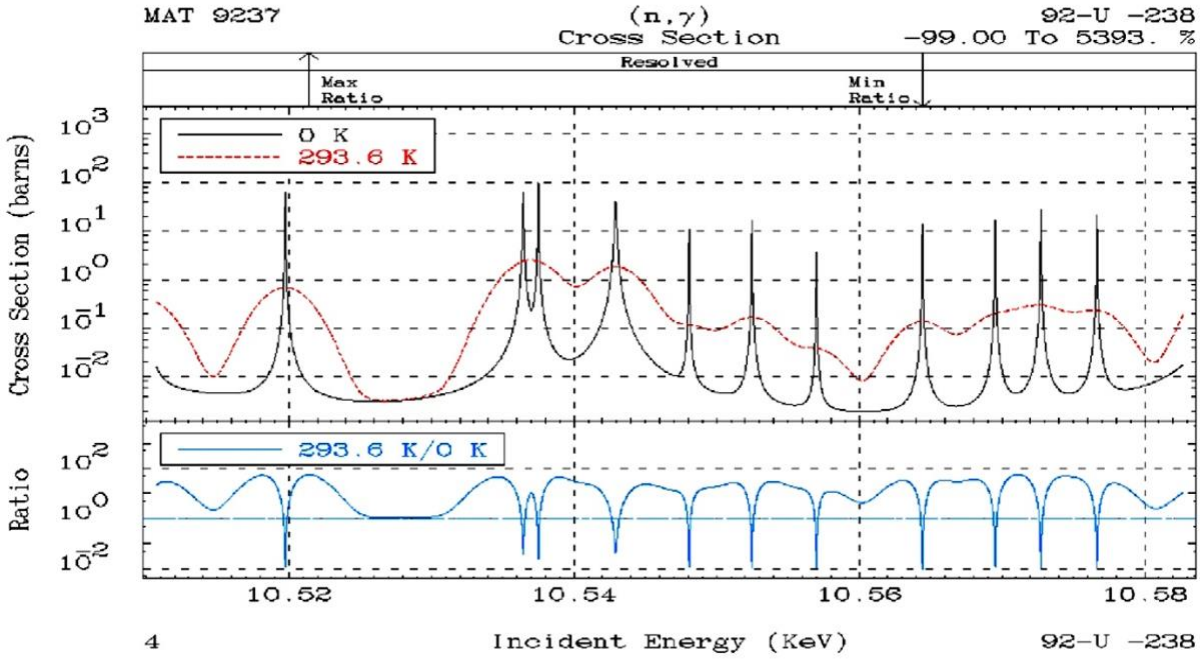

Figure 11 Broadening effects on resonances, zoon in

I will repeat: We cannot uniquely un-Doppler cross sections: **mathematically** the diffusion equation tells us this, and **physics** tells us this would violate the laws of thermodynamics by attempting to create order out of chaos. When we examine the effects of Doppler broadening over a very large temperature range we can see the effect of smoothing the REACTION RATE (neutron speed X cross section) in which eventually all of the resonance structure disappears and we see 1/v cross section, i.e., a smooth, constant REACTION RATE.

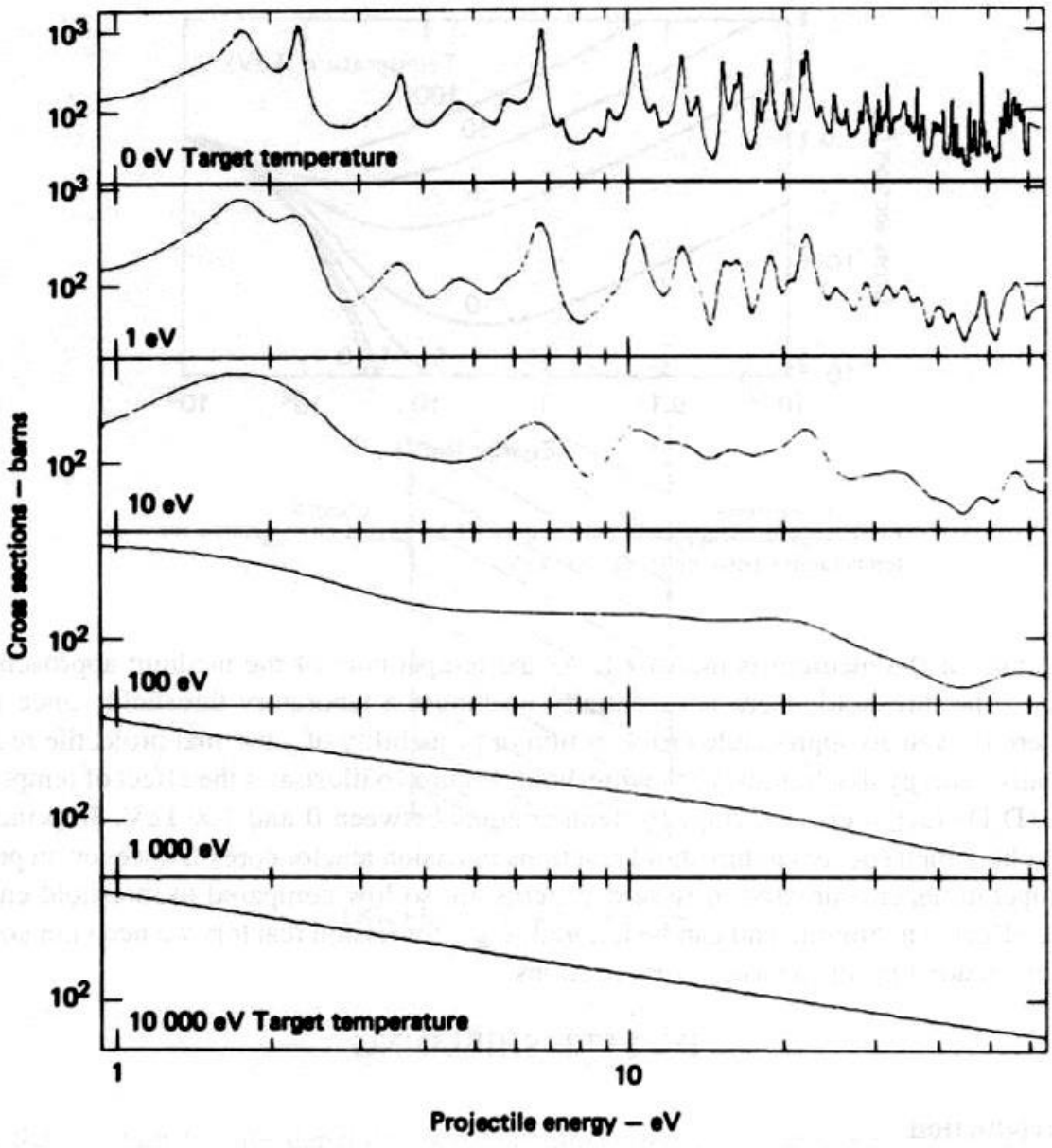

Figure 12 Broadening to high temperatures, T > 1 eV

VI.7 Doppler Broadening at Low Energy

Another effect of temperature, that was often ignored by older Doppler broadening methods, is the effect at low energy. In focusing only on resonances one approximation is to assume that it is the CROSS SECTION, rather than the REACTION RATE, that is being "smoothed". This effect cannot be ignored at low energy. Figure 13 illustrate the hydrogen elastic scattering cross section at 0 and 293.6 K temperature. The "cold" hydrogen cross section at thermal room temperature at 0.0253 eV neutron energy is known accurately to be close to 20 barns. In comparison the "hot", room temperature, cross section is close tom 30 barns, 50% higher. This effect is because at low energy the hydrogen elastic CROSS SECTION is very constant, so the REACTION RATE is increasing in proportion to the speed (v) of a neutron.

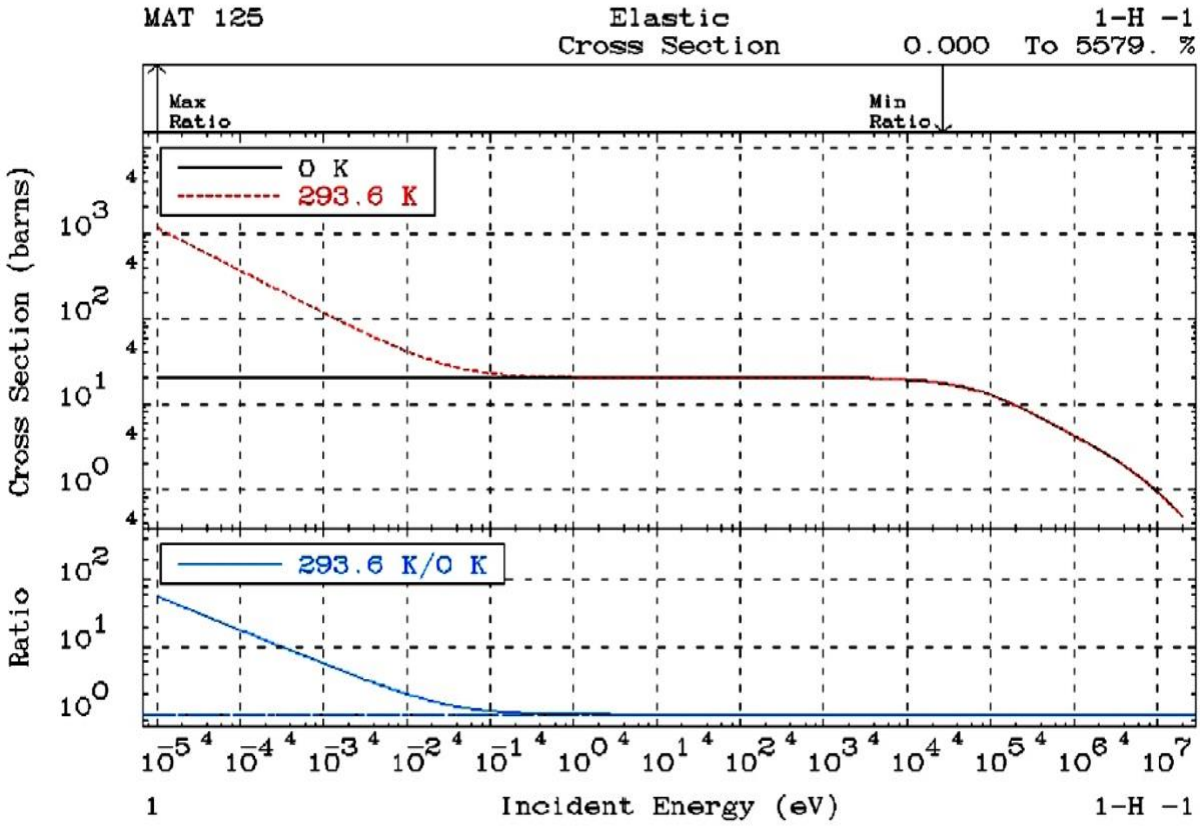

Figure 13 Broadening below 0.1 eV incident, elastic, A = 1

In comparison the hydrogen capture cross section in figure 14 in the thermal range varies as 1/v (inversely as the speed of a neutron), so that the REACTION RATE is constant, and since the reaction rate is already "smooth" we do not expect to see any change with temperature, which is what we see below, i.e., the SIGMA1 method correctly includes both of these effects.

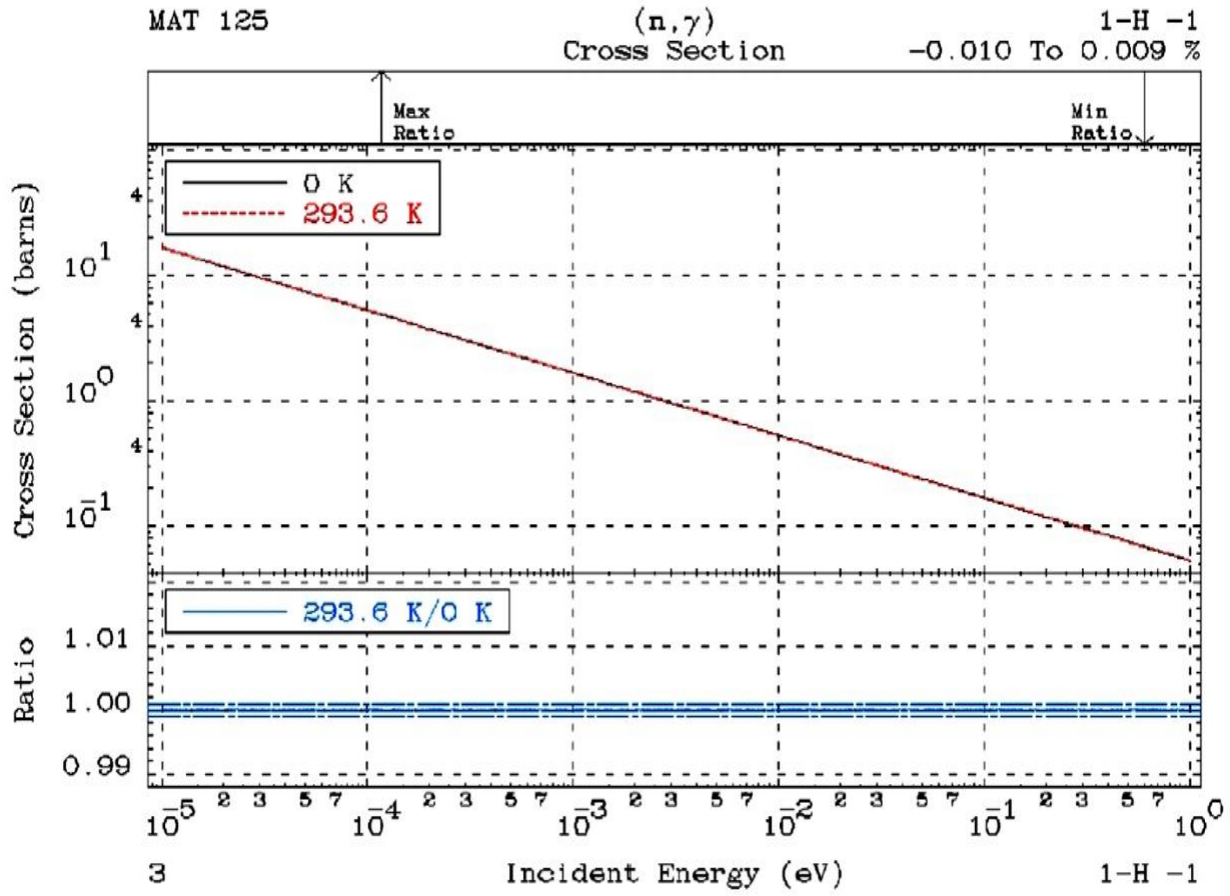

Figure 14 Broadening below 1 eV incident, capture, A =1

The same low energy effects can be seen in figure 15 for U238 elastic and capture at low energy. Again, these figures illustrating the increase in the elastic with temperature and the temperature independent capture. Compared to hydrogen here the effect is at a low neutron energy, because these low energy effects vary approximately as sqrt(KT/AE); T = temperature; A = atomic weight of the target; E = neutron incident energy, e.g., for U238 we expect to see the same effects as for hydrogen roughly 15 times lower in energy, due to the difference in atomic weight (A).

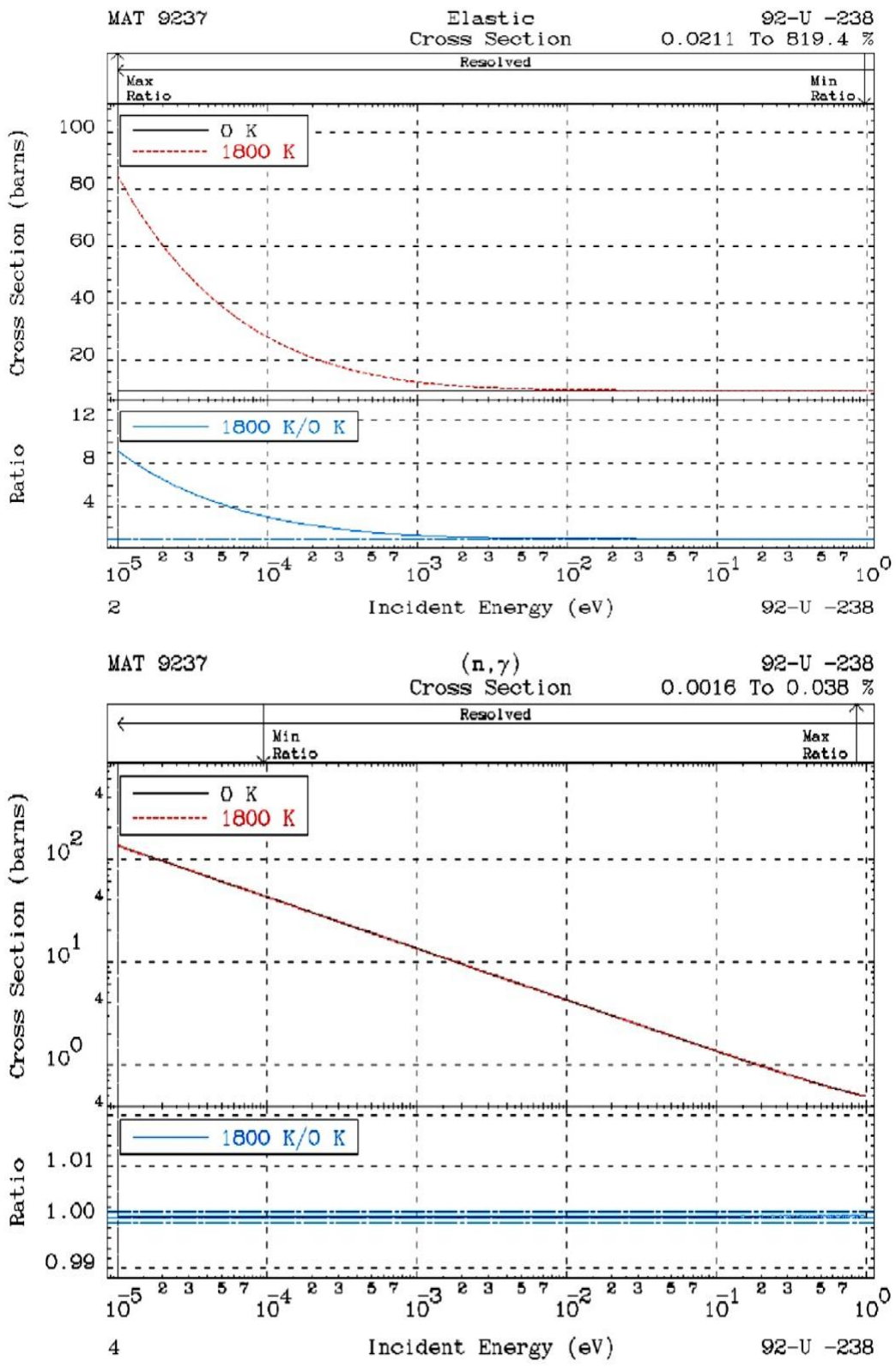

Figure 15 Broadening below 0.001 eV incident, A = 92

VI.8 The Unresolved Resonance Region

Recall that the SIGMA1 method [26] was designed to start from linearly interpolable, tabulated energy dependent free atom cross section in the ENDF format. Based on using the ENDF Pre-Processing codes, PREPRO [25], we have the energy dependent cross sections that SIGMA1 requires at all incident neutron energies, except in the unresolved resonance energy range, where we have tabulated ENERGY AVERAGE UNSHIELDED CROSS SECTIONS. Fortunately, the ENDF-102 convention is that these average values are energy independent, which physically makes sense for broad averages, i.e., at every temperature we have the same numbers of barns in each broad energy range, merely smoother with increasing temperature.

Since these tabulated energy averaged values are defined to be temperature dependent SIGMA1 copies the tabulated values from ENDF input to output without any significant changes. Figure 16 illustrate temperature independence of the U238 elastic and capture cross section at 0 and 1800 K. Be aware that for use in applications, self-shielding of the unresolved resonance region should be included, but this topic is beyond the scope of the discussion here of Doppler broadening.

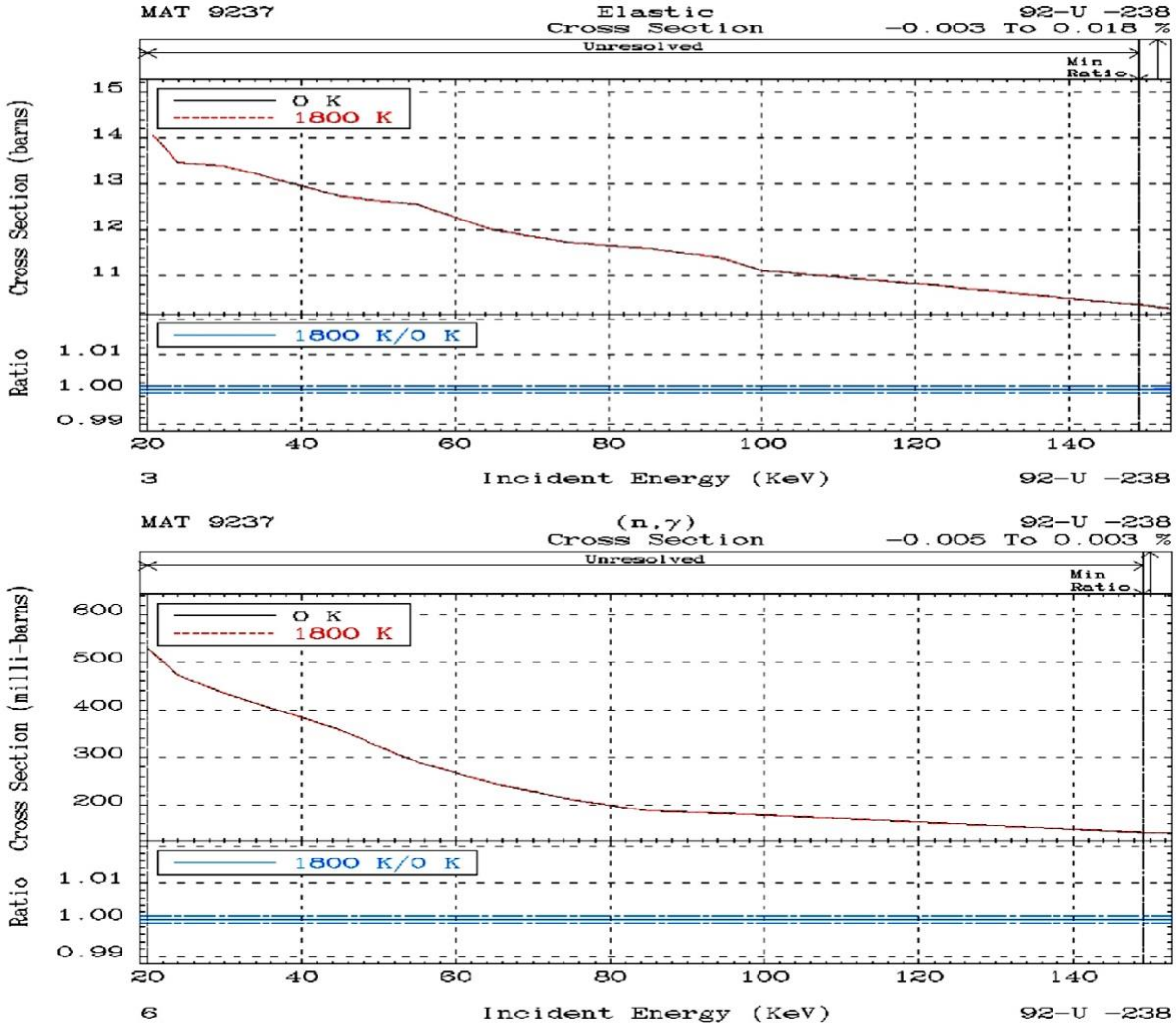

Figure 16 Broadening, unresolved averages

VI.9 Doppler broadening of Thresholds

The apparent Doppler broadening of cross sections is because we perform applications in the laboratory (LAB) system, where the motion of the target nuclei due to thermal motion makes it appear that a neutron traveling at a given LAB frame-of-reference speed has temperature dependent cross sections. In fact, in a relative frame of reference at the temperatures we normally encounter, neutron cross sections are INDEPENDENT of temperature. Indeed, the Doppler broadening equation that we solve has this assumption explicitly built into it.

The bottom line is that for our applications we require LAB system cross sections, and ALL cross sections in the ENDF format are defined to be in the LAB system, Above I illustrated the effect of Doppler broadening on resonances and at low energy, but there is another effect that can be important. Threshold reactions require a minimum energy, or speed, which is uniquely defined in the relative frame of reference. In the LAB system the LAB speed of neutron, which by itself may be below the required threshold speed, and target speed, due to thermal motion, can combine to result in RELATIVE speeds that exceed the threshold.

The result is that in the LAB frame of reference THRESHOLDS ARE TEMPERATURE DEPENDENT, shifting to lower and lower "effective" LAB frame-of-reference threshold energies, with increasing temperature. Figure 17 illustrates the effect of temperature on the (D,D) fusion cross section for temperatures between 0 and 100 keV; this is an important "bootstrap" effect that can result in fusion below the relative frame threshold. In principle a similar phenomenon occurs for threshold reactions in fission reactor. However, in practice the temperatures encountered in fission systems are so low compared to threshold energies that the effect is negligible and can in most cases be ignored, e.g., for fission reactors we need not consider Doppler broadening of inelastic cross sections, or we can easily account for it using a thermal scattering model [27] near the effective threshold.

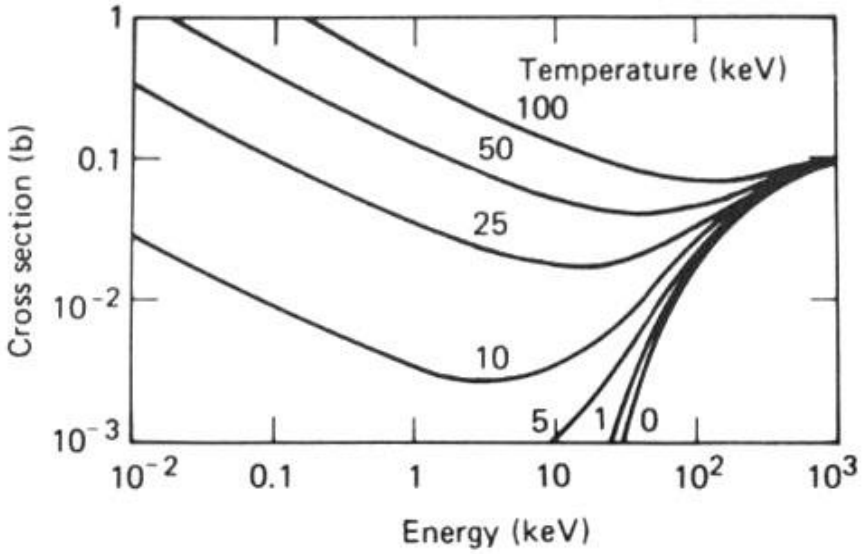

Figure 17 Broadening, threshold reaction above T = 1 eV

VI.10 Doppler Broadening High Energy Cutoff

Today many modern evaluations extend to very high energies, well above the traditional ENDF 20, 30 MeV high energy limit. In these cases, the theoretical models used for the evaluations change at or near 20/30 MeV, which can cause an abrupt change (a non-physical discontinuity) in cross sections; it may be unphysical, but it is what the evaluators intend. To compensate for the "intent" of the evaluators, SIGMA1 Doppler broadening now only extends up to 10 MeV. This has the effect of removing the "smoothing" effect in older versions of SIGMA1 and maintaining the "discontinuities" in the cross section at or near 20/30 MeV. The bottom line is that today all ENDF cross sections above 10 MeV are not broadened by PREPRO/SIGMA1 and are copied from the ENDF input to ENDF output, exactly as input.

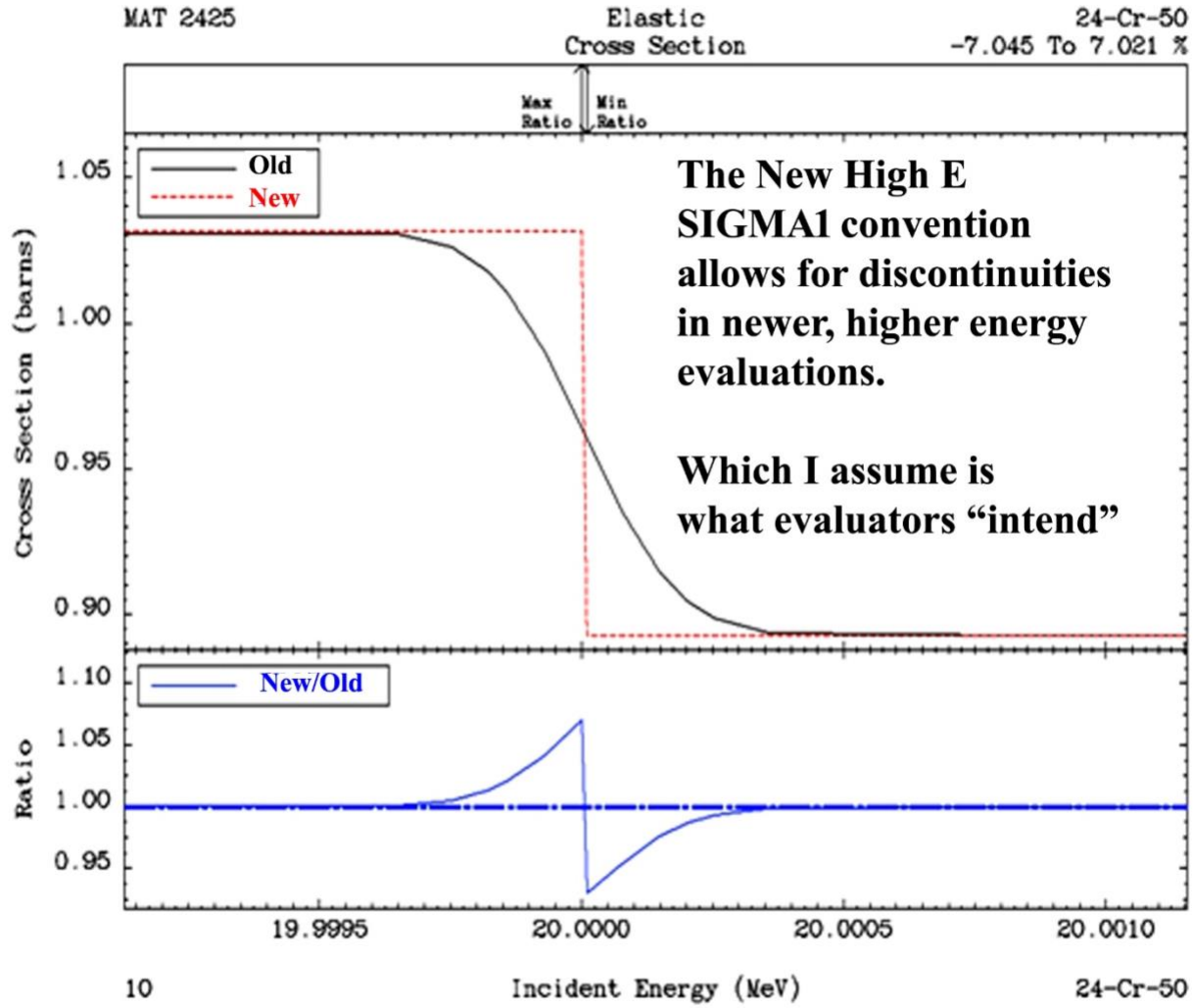

Figure 18 Transition energy discontinuity processing interpretation effect

VI.11 Ensure Doppler Broadening extends to High Enough Energy

Unfortunately, some codes that use the SIGMA1 method do not appear to understand how high up in energy the effects of Doppler broadening extend, and they only extend Doppler broadening to relatively low energies, and as such they are not accounting for temperature effects at high energy. It may come as a surprise when you read in the above section that SIGMA1 Doppler broadening extends up to 10 MeV.

Based on decades of data testing we now understand the problem created by codes that failure to continue Doppler broadening to high enough incident neutron energies: 1) Today extending to high energy increases computer processes by very little, because beyond the resolved resonance region there are relatively few tabulated cross sections, 2) Failure to broaden to higher temperatures can result in ignoring important effects.

Figure 19 illustrate Doppler broadening Fe56 total cross section comparing 0 and 293.6 K, i.e., merely from cold to room temperature. Through the resolved resonance region, we see major effects to above 800 keV. In the second figure we see smaller, but not insignificant effects of broadening above the resolved resonance region, all the way up to 9 MeV.

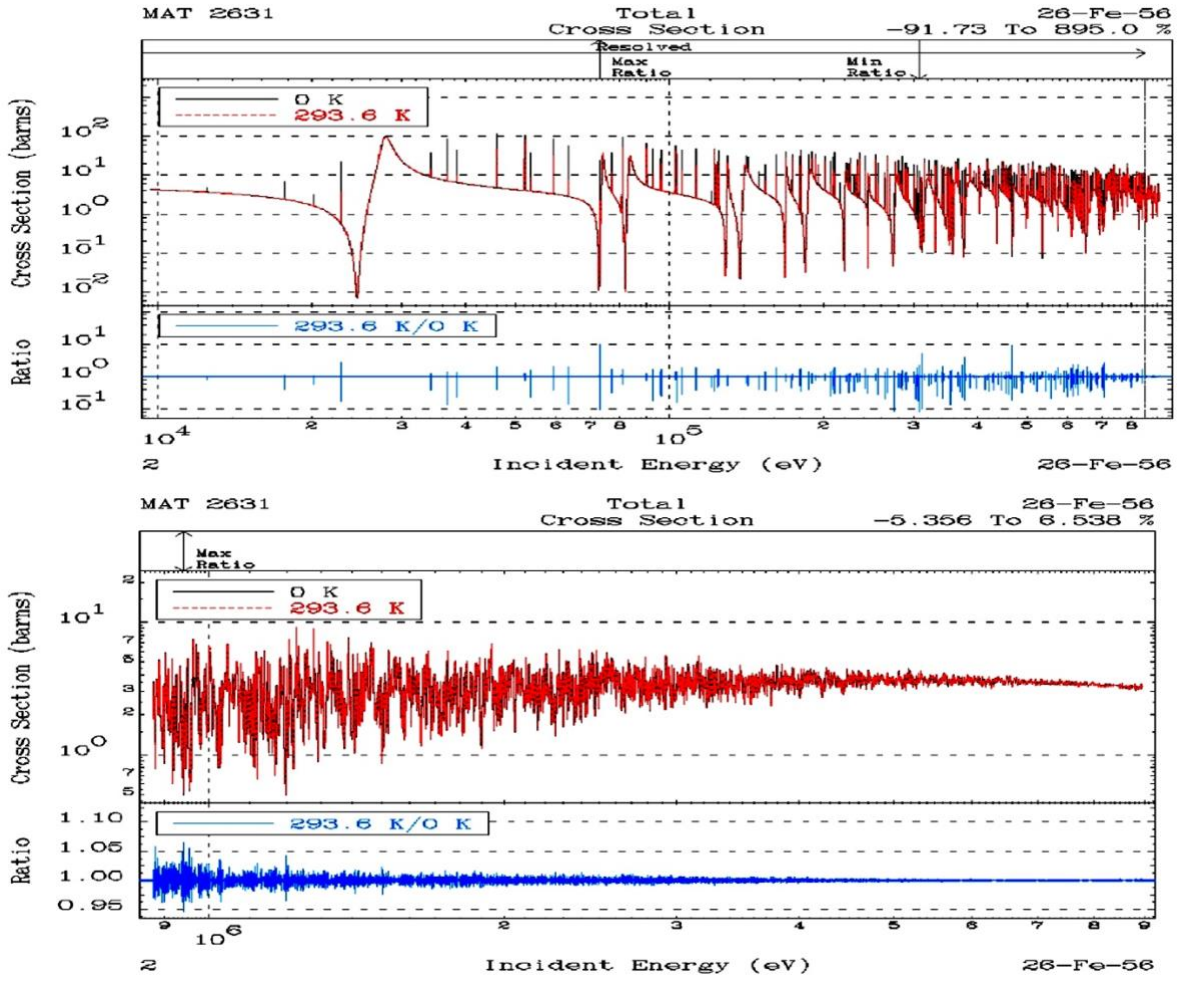

Figure 19 Broadening structures up to 10 MeV incident

VI.12 Thermal Scattering Law

The SIGMA1 method is designed to Doppler broaden FREE ATOM nuclear data. It is not designed to handle BOUND ATOMS, as we find in Thermal Scattering Law data [27]. Figure 20 show a few examples comparing FREE ATOM and BOUND ATOM data. Hopefully, from these figures you will realize that SIGMA1 MUST NOT be used to broaden bound data. Free atom data in the relative frame of reference is INDEPENDENT of temperature, and can be defined by the diffusion equation, which is what the SIGMA1 method assumes. In contrast, bound atom data can be temperature DEPENDENT and its temperature dependence is defined by completely different physics. As such it is beyond the scope of the SIGMA1 method and this report.

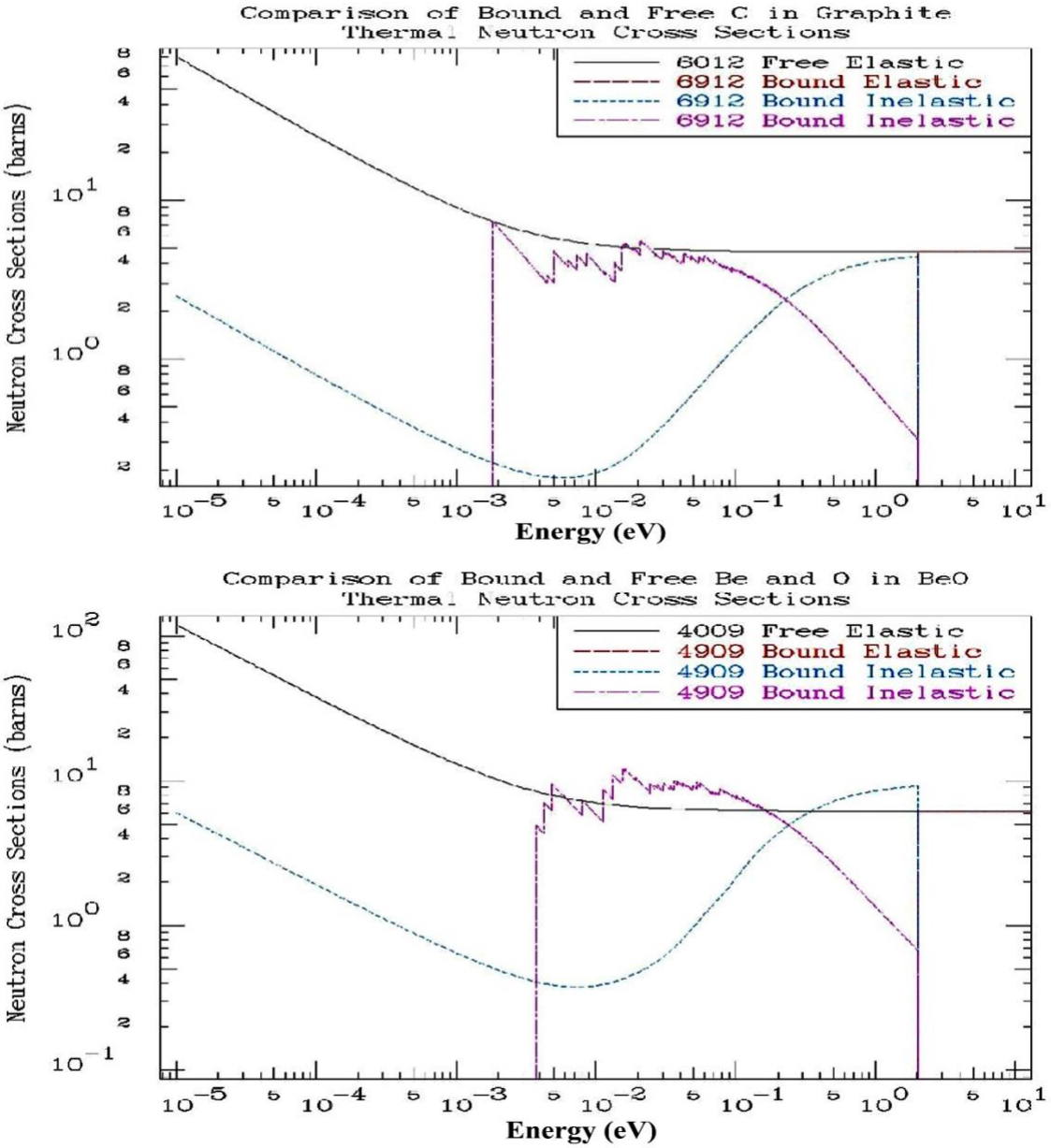

Figure 20 Thermal motion below 10 eV incident

VI.13 Self-Shielding

Integral effects of temperature are so important I will repeat some subject already discussed in this report. An important integral effect of temperature is its effect on self-shielding; this is an inherently energy integral effect. Neutron flux is the distance traveled by neutrons per unit time and volume. So, it should not come as a surprise to realize that doubling the total cross sections halves the distance traveled by neutrons between collisions. This means that resonances, in which we see rapid increases – and decreases – in the cross section, cause rapid swings in the flux in the opposite direction; this is called "self-shielding", because it is the resonances that shield themselves against the flux.

To understand the importance of considering temperature we should consider reaction rates, such as captures/second, in various systems. In optically thin systems (few mean free paths dimensions) the flux will be unshielded, and our reaction rates will be defined by a simple cross section average,

Unshielded Capture = $\int_{E1}^{E2}[\Sigma c(E)\phi(E)]dE$ = capture cross section times neutron flux

In optically thick systems (many mean free paths dimensions) the flux will be shielded (the flux is suppressed by the total cross section) and our reaction rates must include the effect of self-shielding on the cross section average,

Shielded Capture = $\int_{E1}^{E2}[\Sigma c(E)\phi(E)/\Sigma t(E)]dE$ = including one over total cross section

Consider for example the U238 capture cross section in the incident neutron energy between 1 and 10 keV as shown above in fig. 5. If we calculate the unshielded and shielded average capture cross section for the energy interval over the range of temperatures shown in figs 5, we obtain the results shown below in the below table.

From the below results we see that the unshielded average capture cross section is virtually independent of temperature, being about 1 barn over the entire temperature range. In contrast the shielded average cross section varying by over a factor of three between the 0 K average (0.293 barns) and the 10 keV average (0.939 barns). The point to learn from this is that without including the effect of self-shielding in multi-group calculations, temperature has very little effect on the average cross sections, which is quite simply wrong for optically thick systems, e.g., a nuclear reactor.

Temp.	Unshielded	Shielded (barns)
0 K	0.996	0.293
293.6 K	0.966	0.526
600 K	0.996	0.576
1,200 K	0.996	0.630
12,000 K (1 eV)	0.996	0.799
10 eV	0.998	0.905
100 eV	1.000	0.933
1 keV	1.004	0.935
10 keV	1.007	0.939

VI.14 Spectral Shift

Above we discussed the effect of temperature on the energy dependence of the laboratory frame-of-reference neutron cross sections, and energy integrated self-shielding. It is important to understand that temperature also has an effect on any entire system by shifting the thermal neutron spectrum. If we again assume a Maxwellian thermal distribution we can see this effect in figure 21 illustrating the spectra in a U/Water spherical system [29].

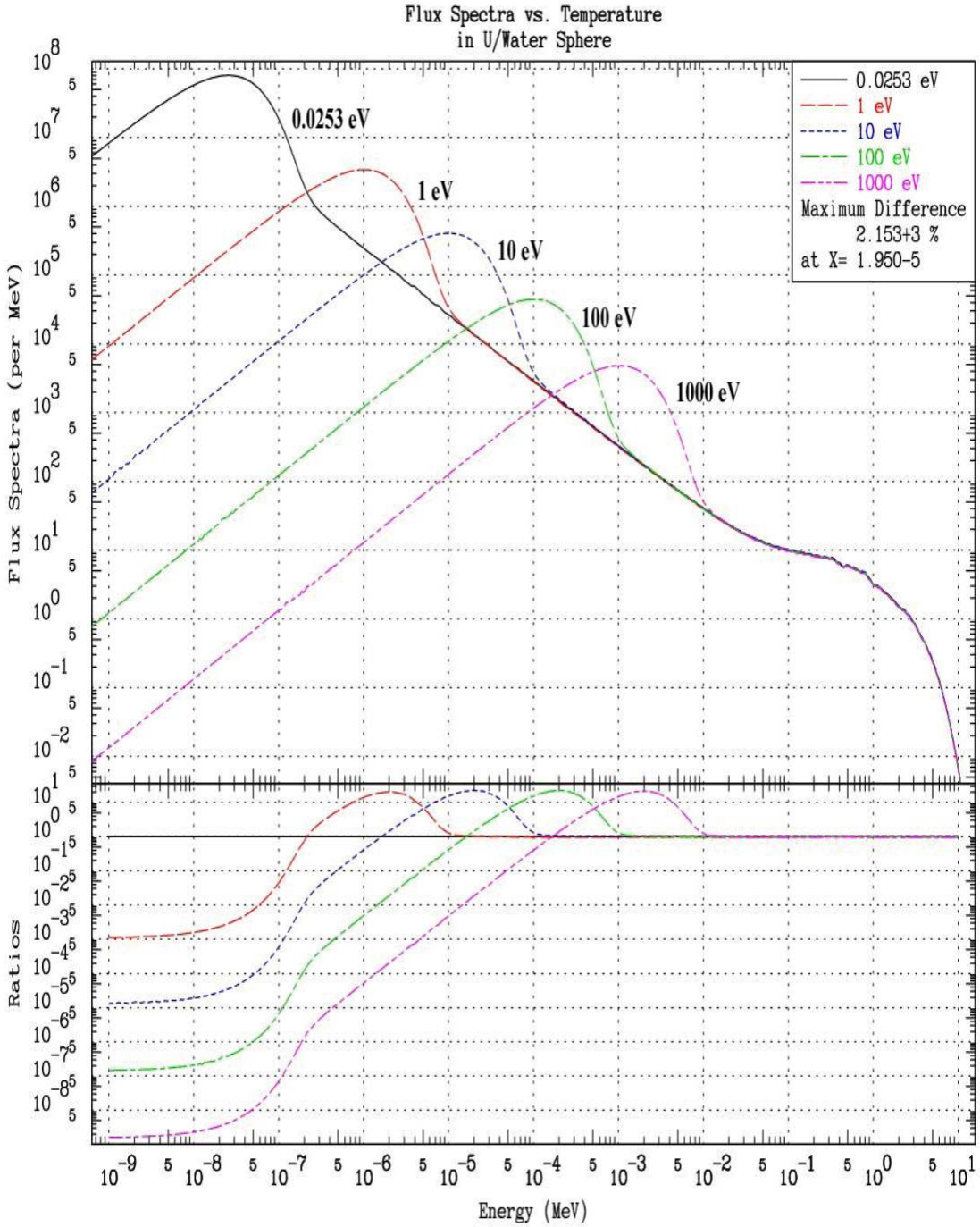

Figure 21 Neutron flux spectra versus temperature

VI.15 Doppler Coefficient

Finally, we will briefly mention the importance of correctly modeling all these temperature effects in order that we can accurately calculate the Doppler coefficient of any system**.** The doppler coefficient defines whether or not any system is stable under a change in temperature. To be stable we require that the reactivity of the system decreases as the temperature increases; otherwise, we would have a dangerous situation where the system could run away, out of control.

Temp.	Unshielded	Shielded (barns)
0 K	0.996	0.293
293.6 K	0.966	0.526
600 K	0.996	0.576
1,200 K	0.996	0.630
12,000 K (1 eV)	0.996	0.799
10 eV	0.998	0.905
100 eV	1.000	0.933
1 keV	1.004	0.935
10 keV	1.007	0.939

See the above results under Self-Shielding for an example of the U238 capture cross section between 1 and 10 keV (reproduced here, for convenience). In this example the shielded capture (as in an optical thick system, such as a fission reactor), increases with the temperature, thereby contributing to a negative Doppler coefficient.

VII. References

[1] A. Koning, S. Hilaire, and S. Goriely. "**TALYS-1.95**, User Manual." (2019). http://www.talys.eu/

[2] D. Rochman , A.J. Koning, J. Kopecky, J.-C. Sublet , P. Ribon , M. Moxon, From average parameters to statistical resolved resonances, Annals of Nuclear Energy 51 (2013) 60–68 https://www.sciencedirect.com/science/article/pii/S0306454912003350

[3] D. Rochman, A.J. Koning, J.-Ch. Sublet "A Statistical Analysis of Evaluated Neutron Resonances with **TARES** for JEFF-3.3, JENDL-4.0, ENDF/B-VIII.0 and TENDL-2019", Nucl. Data Sheets 163 (2020) 163-190.

[4] A.J. Koning, D. Rochman, J.-Ch. Sublet, N. Dzysiuk, M. Fleming and S. van der Marck, "**TENDL:** Complete Nuclear Data Library for Innovative Nuclear Science and Technology", Nuclear Data Sheets 155 (2019)
https://www.sciencedirect.com/science/article/abs/pii/S009037521930002X

[5] A. Koning and D. Rochman. "**TENDL-2019**: TALYS-based Evaluated Nuclear Data Library, (2019) https://tendl.web.psi.ch/tendl_2019/tendl2019.html

[6] **TENDL-2019** forms for applications: https://tendl.web.psi.ch/tendl_2019/tar.html

[7] J.-Ch. Sublet, J. W. Eastwood, J. G. Morgan, M. R. Gilbert, M. Fleming, W. Arter. **FISPACT-II:** An Advanced Simulation System for Activation, Transmutation and Material Modelling. Nuclear Data Sheets 139 (2017) 77-137 and https://fispact.ukaea.uk/

[8] J.W. Eastwood, J.G. Morgan, J.-Ch. Sublet, Inventory Uncertainty Quantification using **TENDL** Covariance Data in Fispact-II, Nuclear Data Sheets Volume 123, January 2015, Pages 84-9 https://doi.org/10.1016/j.nds.2014.12.015

[9] H. Bateman, The Solution of a System of Differential Equations Occurring in the Theory of Radio-active Transformations, Proc. Camb. Phil. Soc., 16, 423 (1910)

[10] C.J. Werner (editor), "**MCNP** User's Manual - Code Version 6.2", LA-UR-17-29981 (2017)

[11] E. Brun, F. Damian, C.M. Diop, E. Dumonteil, F.X. Hugot, C. Jouanne, Y.K. Lee, F. Malvagi, A. Mazzollo, O. Petit, J.C. Trama, T. Visonneau, A. Zoia, **Tripoli-4**®, CEA, EDF and AREVA reference Monte Carlo code, Annals of Nuclear Energy 82, 151-160 (2015) and http://www.cea.fr/tripoli-4/

[12] J. Leppanen et al. "The **Serpent** Monte Carlo code: Status, development and applications in 2013." Ann. Nucl. Energy, 82 (2015) 142-150 (2015)

[13] P.K. Romano, N. E. Horelik, B. R. Herman, A. G. Nelson, B. Forget, and K. Smith, "OpenMC: A State-of-the-Art Monte Carlo Code for Research and Development," Ann. Nucl. Energy, 82, 90–97 (2015) and https://docs.openmc.org/en/stable/

[14] Studsvik, **CASMO5**, https://www.studsvik.com/our-solutions/products/casmo/

[15] M. Gilbert and J.-Ch. Sublet, Differential dpa calculations with **SPECTRA-PKA**, J. Nucl. Mater. 504 (2018) 101-108 and http://fispact.ukaea.uk/wiki/Spectra-PKA

[16] JANIS Books: **TENDL versus EXFOR** https://www.oecd-nea.org/janis/book/ and https://tendl.web.psi.ch/tendl_2019/tendl2019.html

[17] **TENDL-2019** Verification and Validation: https://fispact.ukaea.uk/documentation-2/reports/ and https://tendl.web.psi.ch/tendl_2019/other/k.pdf and https://www-nds.iaea.org/CRPdpa/

[18] **POINT 2003:** A Temperature Dependent ENDF/B-VI, Release 8, Cross Section Library, Lawrence Livermore National Laboratory, CA (US), UCRL-ID-127776-Rev-2, May 2003.

[19] **POINT 2007:** A Temperature Dependent ENDF/B-VII.0 Data Cross Section Library, Lawrence Livermore National Laboratory, UCRL-TR-228089, February 2007.

[20] **POINT 2011:** A Temperature Dependent ENDF/B-VII.0 data Cross Section Library, Lawrence Livermore National Laboratory, UCRL-TR-479947, rev. 1, May 2011.

[21] **POINT 2015**: ENDF/B-VII.1 Final Temperature Dependent Cross Section Library, IAEA-NDS-221, IAEA, Vienna, Austria, March 2015.

[22] **POINT 2018**: ENDF/B-VIII Final Temperature Dependent Cross Section Library", IAEA-NDS-227, April 2018, Nuclear Data Section (NDS), IAEA, Vienna, Austria.

[23] **ENDF/B-VIII.0**: The 8th Major Release of the Nuclear Reaction Data Library with CIELO-project Cross Sections, New Standards and Thermal Scattering Data, D.A.Brown, et.al. Nucl. Data Sheets 148 (2018) 1-142.

[24] **ENDF-102:** ENDF-6 Formats Manual: Data Formats and Procedures for the Evaluated Nuclear Data Files ENDF/B-VI, ENDF/B-VII and ENDF/B-VIII, BNL-203218-2018-INRE, Rev. 215, Feb. 2018, edited by A. Trkov, M. Herman and D. A. Brown, National Nuclear Data Center, Brookhaven National Lab. http://www.nndc.bnl.gov/csewg/docs/endf-manual.pdf

[25] **PREPRO2019**: 2019 ENDF/B Pre-processing Codes (ENDF/B-VIII Verified)", IAEA-NDS-229. Nuclear Data Section, IAEA, Vienna, Austria, August 2019; PREPRO2020 is planned for public release later in 2020. https://www-nds.iaea.org/public/endf/prepro/

[26] **Exact Doppler Broadening** of Tabulated Cross Sections, by D.E. Cullen and C.R. Weisbin, Nucl. Sci. Eng. 60 (1976) 199.

[27] **THERMAL**: A Routine Designed to Calculate Neutron Thermal Scattering, by D.E. Cullen, Lawrence Livermore National Laboratory, UCRL-ID-120560-Rev-1, Sept. 1995.

[28] "**Nuclear Data Preparation**", pp. 279-425, Vol. 1, in "The Handbook of Nuclear Engineering", Springer Publishing, NY, NY (2010)

[29] **TART 2016**: An Overview of a Coupled Neutron-Photon 3-D, Combinatorial Geometry Time Dependent Monte Carlo Transport Code, Report: LLNL-SM-704560, Code Release: LLNL-CODE-708759, September 2016. https://e-reports-ext.llnl.gov/pdf/837508.pdf

[30] Greene, N.M., et al., "**AMPX**: A Modular Code System for Generating Coupled Multigroup Neutron-Gamma Libraries from ENDF/B", ORNL-TM-3706, Oak Ridge National Laboratory, Oak Ridge, Tenn., 1976

[31] Hutchins, B.A., et al., "**ENDRUN-II**, A Computer Code to Generate a Generalized Multigroup Data File from ENDF/B", GEAP-13704 (ENDF-145), General Electric Company, Sunnyvale, CA, 1973.

[32] Green, D.M., and Pitterle, T.A., "**ETOE**, A Program for ENDF/B to MC2 Data Conversion", APDA-219 (ENDF-120), Atomic Power Development Associates, Inc., 1968.

[33] Gregson, K. and James, M.F., "**TEMPO**-A General Doppler Broadening Program for Neutron Cross Sections", AEEW-M518, U.K. Atomic Energy Establishment, Winfrith, England, 1965.